Title

The prenucleosome, a stable conformational isomer of the nucleosome

Journal

Genes and Development, 29(24)

ISSN

0890-9369

Authors

Fei, J

Torigoe, SE

Brown, CR

et al.

Publication Date

2015-12-15

DOI

10.1101/gad.272633

Peer reviewed

The Prenucleosome, a Stable Conformational Isomer of the Nucleosome

Jia Fei[1], Sharon E. Torigoe[1], Christopher R. Brown[2], Mai T. Khuong[1], George A. Kassavetis[1], Hinrich Boeger[2], and James T. Kadonaga[1,3]

[Key words: Nucleosome, Prenucleosome, Active Chromatin, Histones, Gene Expression]

Running Head: Conformational Isomer of the Nucleosome

[1]Section of Molecular Biology, University of California, San Diego, La Jolla, CA 92093, USA.

[2]Department of Molecular, Cell and Developmental Biology, University of California, Santa Cruz, Santa Cruz, CA 95064, USA.

[3]Corresponding author. Email: jkadonaga@ucsd.edu

Chromatin comprises nucleosomes as well as non-nucleosomal histone-DNA particles. Prenucleosomes are rapidly formed histone-DNA particles that can be converted into canonical nucleosomes by a motor protein such as ACF; however, the composition of the prenucleosome and its relation to the nucleosome are not known. Here we show that the prenucleosome is a stable alternate conformational isomer of the nucleosome. It consists of a histone octamer associated with about 80 bp DNA, which is located at a position that corresponds to the central 80 bp of a nucleosome core particle. Monomeric prenucleosomes with free flanking DNA do not spontaneously fold into nucleosomes, but can be converted into canonical nucleosomes by an ATP-driven motor protein such as ACF or Chd1. In addition, histone H3K56, which is located at the DNA entry and exit points of a canonical nucleosome, is specifically acetylated by p300 in prenucleosomes relative to nucleosomes. Prenucleosomes assembled in vitro exhibit properties that are strikingly similar to those of non-nucleosomal histone-DNA particles in the upstream region of active promoters in vivo. These findings suggest that the prenucleosome, the only known stable conformational isomer of the nucleosome, is related to non-nucleosomal histone-DNA species in the cell.

Chromatin in the eukaryotic nucleus consists of nucleosomes and non-nucleosomal particles. Nucleosomes have been extensively studied and are well understood. In contrast, little is known about non-nucleosomal chromatin particles. These species are likely to be biologically important because they are found in regions of active chromatin such as promoters. One might imagine canonical nucleosomes as the static component of chromatin and non-nucleosomal particles as the dynamic component of chromatin.

We recently discovered a non-nucleosomal chromatin particle termed the prenucleosome, which is a precursor to the nucleosome in the assembly of chromatin (Torigoe et al. 2011, 2013; Bouazoune and Kingston 2013). Prenucleosomes contain all four core histones, do not supercoil DNA like a canonical nucleosome, and can be converted into periodic nucleosome arrays by an ATP-dependent chromatin assembly motor protein such as ACF or Chd1. By atomic force microscopy, prenucleosomes are indistinguishable from canonical nucleosomes. In addition, prenucleosomes are rapidly formed within seconds, are stable and resistant to challenge by free DNA for at least two hours, and are more sensitive to digestion by micrococcal nuclease (MNase) than canonical nucleosomes.

The discovery of prenucleosomes provided a resolution to a paradox from the 1970s. At that time, it was observed that nucleosome-like structures (containing at least histones H3 and H2B) form within seconds upon passage of DNA replication forks (see, for example: McKnight and Miller 1977; McKnight et al. 1978; Sogo et al. 1986), whereas canonical "mature" nucleosomes, as characterized by nuclease digestion and sedimentation properties, are more slowly generated after approximately 10 to 20 min (see, for example: Seale 1975, 1976; Levy and Jakob 1978; Worcel et al. 1978; Schlaeger and Knippers 1979; Klempnauer et al. 1980; Jackson and Chalkley 1981). Thus, the question was – how could nucleosome-like particles be formed within seconds when it was also known that it takes at least 10 min to form a canonical nucleosome? It now appears that this paradox can be explained by the rapid formation of prenucleosomes at DNA replication forks.

Because prenucleosomes are formed rapidly, they can provide immediate protection of naked DNA that might be generated during processes such as replication and transcription. In addition, prenucleosomes or prenucleosome-like particles might function, such as at promoters and enhancers, as a more dynamic (less static and repressive) form of histone-bound DNA than canonical nucleosomes.

We do not yet know what a prenucleosome is. Does it contain a histone octamer or some other combination of the histones? How much DNA is associated with a prenucleosome, and where is the DNA located relative to the histone octamer? Why do prenucleosomes not supercoil DNA like nucleosomes? In previous work, we assembled prenucleosomes onto relaxed plasmid DNA (Torigoe et al. 2011). While this approach has been useful for the characterization of the function of prenucleosomes in the chromatin assembly process, the resulting templates were heterogeneous in terms of the number and locations of the prenucleosomes. Hence, with that system, it was not possible to determine the composition and structure of the prenucleosome.

In this study, we have taken a new experimental approach to the analysis of prenucleosomes and have determined that the prenucleosome is a stable alternate conformational isomer of the nucleosome. We have further found that the properties of prenucleosomes assembled in vitro are remarkably similar to those of non-nucleosomal histone-DNA particles at active promoters in vivo. The prenucleosome is the only known stable alternate conformer of the nucleosome. Because there are probably only a limited number of alternate conformations of the nucleosome, prenucleosomes may share a common fundamental structure with native non-nucleosomal particles such as those present at active chromatin throughout the genome.

Results

Electron microscopy reveals that prenucleosomes associate with approximately 70-80 bp DNA – the same as that seen with chromatin particles at active promoters in vivo

To investigate the properties of prenucleosomes, we employed psoralen crosslinking and electron microscopy analysis. This method was originally developed for the study of nucleosomes and involves psoralen crosslinking of the linker DNA between nucleosomes followed by electron microscopy under denaturing conditions. The segments of DNA that are bound by histones appear as bubbles of single-stranded DNA (Hanson et al. 1976; Sogo et al. 1986; Brown et al. 2013, 2015).

In our studies of prenucleosomes, we carried out chromatin assembly reactions with relaxed plasmid DNA in the absence or presence of ACF to give prenucleosomes or canonical nucleosomes, and the resulting samples were subjected to psoralen crosslinking, linearization, and electron microscopy. Representative images of the bubbles observed with prenucleosomes and nucleosomes are shown in Fig. 1A. Quantitation of the number of bubbles per plasmid DNA revealed approximately the same number of prenucleosomes and nucleosomes per template (Fig. S1). This finding is consistent with our previous analysis of prenucleosomes and nucleosomes by atomic force microscopy (Torigoe et al. 2011). The measurement of the bubble sizes revealed a peak at 140-150 nt with canonical nucleosomes, as expected. With prenucleosomes, however, we observed a peak at about 70-80 nt (Fig. 1B) as well as larger bubbles that may have been due to the presence of some canonical nucleosomes in the predominantly prenucleosomal samples (as in Torigoe et al. 2011). These findings suggest that prenucleosomes associate with approximately 70-80 nt of DNA, which corresponds to less than one turn of the DNA around the histone octamer in a nucleosome. This partial wrapping of DNA around the histones in prenucleosomes (relative to that in nucleosomes) might explain the lack of DNA supercoiling that is observed during the formation of prenucleosomes (Torigoe et al. 2011).

These studies additionally enabled us to compare the properties of prenucleosomes assembled in vitro and non-nucleosomal chromatin particles observed in vivo. Remarkably, the biochemical data on prenucleosomes versus nucleosomes (Fig. 1B) exhibit a close resemblance to the psoralen bubble size distribution observed in vivo with the active versus repressed *PHO5* promoter in yeast (Brown et al. 2013). In the in vivo analysis, a peak bubble size of 70-80 bp DNA was seen at the activated *PHO5* promoter, whereas a peak of 140-150 bp was observed at the repressed *PHO5* promoter. To demonstrate the correlation, we directly compared the in vitro data (this study) and in vivo data (Brown et al. 2013) (Fig. 1C). These data suggest that the active *PHO5* promoter contains both prenucleosomes (or prenucleosome-like particles) and nucleosomes, whereas the repressed *PHO5* promoter contains mostly canonical nucleosomes. Thus, although prenucleosomes were initially identified in the analysis of chromatin assembly, these findings indicate that they may also be present at the promoter regions of active genes.

Rapid and efficient assembly of monomeric prenucleosomes onto 80 bp DNA fragments

The psoralen crosslinking and electron microscopy experiments additionally led to a new approach to the analysis of prenucleosomes. If prenucleosomes associate with 70-80 bp of DNA, we thought that it might be possible to assemble a monomeric prenucleosome with histones and an 80 bp DNA fragment. To test this hypothesis, we deposited core histones onto an 80 bp DNA fragment by using the NAP1 core histone chaperone. We employed the same conditions as those used for the formation of prenucleosomes on plasmid DNA templates (Torigoe et al. 2011), except that a short 80 bp DNA fragment was used instead of relaxed plasmid DNA. These experiments revealed the rapid (complete within 30 s) formation of a distinct nucleoprotein species with all four core histones (Fig. 2A). There was essentially complete conversion of the free DNA to the nucleoprotein species at a 1:1 histone octamer:DNA ratio. Under these same conditions, we did not see the efficient formation of distinct complexes with equimolar amounts of either H3-H4 or H2A-H2B. Based on these data and other results

shown later in this work, we refer to these nucleoprotein complexes as monomeric prenucleosomes, or "mono-prenucleosomes".

We then tested whether mono-prenucleosomes can be assembled with different DNA segments. In Fig. 2A, we used an 80 bp stretch of DNA from the coding sequence of the *Drosophila melanogaster ISWI* gene (sequence given in Table S1) – we will refer to this fragment as the "80 bp genomic DNA". We have also used the central 80 bp of the 601 nucleosome positioning sequence (Lowary and Widom 1998; sequence given in Table S1) – we term this fragment the "central 80 bp of 601 sequence". As shown in Fig. 2B, mono-prenucleosomes can be formed efficiently with either the 80 bp genomic DNA or the central 80 bp of 601 sequence. These two DNA fragments are used throughout this study.

Next, we sought to determine whether mono-prenucleosomes are generally formed under different reaction conditions. To this end, we tested a different core histone chaperone, *Drosophila* nucleoplasmin-like protein (dNLP; Ito et al. 1996), as well as salt dialysis techniques (Stein 1989) for the reconstitution of mono-prenucleosomes. These experiments revealed that mono-prenucleosomes are efficiently formed not only with NAP1, but also with dNLP and by salt dialysis in the absence of histone chaperones (Fig. 2C). Thus, in a minimal purified reaction consisting only of the four core histones and 80 bp DNA, mono-prenucleosomes can be formed by salt dialysis under standard conditions used for nucleosome reconstitution, in which the histones and DNA are combined in 1 M NaCl and the samples are slowly dialyzed in a stepwise manner to 0.05 M NaCl (Stein 1989). These results indicate that the mono-prenucleosome is a thermodynamically stable arrangement of the four core histones and 80 bp DNA.

It should also be noted that mono-prenucleosome reconstitution requires a histone chaperone, such as NAP1 or dNLP, or initial high salt conditions that prevent the formation of histone-DNA aggregates. If core histones are added directly to free DNA in low salt buffer (for example, with 100 mM NaCl or less), insoluble histone-DNA aggregates are formed that do not enter the gel (Fig. 2C).

Comparison of assembly by salt dialysis with all four core histones or equimolar amounts of histones H3-H4 reveals the efficient formation of mono-prenucleosomes with the four core histones and inefficient formation of mono-tetrasomes with histones H3-H4 (Fig. 2C). Moreover, we observed that mono-tetrasomes can be efficiently converted into mono-prenucleosomes by the addition of NAP1-H2A-H2B complexes (Fig. 2D). These findings reveal that mono-tetrasomes are distinct from mono-prenucleosomes.

Analysis of the composition and salt lability of mono-prenucleosomes

We then analyzed the composition of mono-prenucleosomes by sucrose gradient sedimentation analysis. In these experiments, mono-prenucleosomes were reconstituted either by NAP1 deposition or by salt dialysis, and then subjected to 10-30% sucrose gradient sedimentation. The presence of mono-prenucleosomes was detected by native gel electrophoresis of the nucleoprotein complexes, as in Fig. 2, and the histones were detected by SDS-polyacrylamide gel electrophoresis and silver staining. These experiments revealed that mono-prenucleosomes co-sediment with all four core histones (Fig. 3A). As a control, histones in mono-prenucleosomes sediment faster than free histones (Fig. S2A). In addition, it can be seen that the sedimentation rate of NAP1-assembled mono-prenucleosomes is the same as that of salt dialysis-reconstituted mono-prenucleosomes (Fig. 3A). Throughout this study, we have found that mono-prenucleosomes that are prepared by either method have the same biochemical properties.

Although the four core histones can be seen in mono-prenucleosomes (Fig. 3A), it was possible that the histones in mono-prenucleosomes exist as a hexamer (with two copies of H3 and H4 and only one copy of H2A and H2B) rather than as an octamer (with two copies each of H2A, H2B, H3, and H4) (see, for example, Arimura et al. 2012). To test the hexamer hypothesis, we reconstituted mono-prenucleosomes with a 3:1 molar ratio of wild-type H2A to Strep-tagged H2A along with the other three core histones at a 1:1:1:1 ratio of total H2A (wild-type H2A + Strep-H2A):H2B:H3:H4. We then pulled down the mono-prenucleosomes

containing Strep-tagged H2A and examined whether wild-type H2A co-precipitates with Strep-H2A by western blot with antibodies against H2A (Fig. 3B). If there were a hexamer of histones in a mono-prenucleosome, then wild-type H2A would not co-precipitate with the Strep-H2A because of the single copy of H2A in a hexamer. However, these experiments revealed the presence of two copies of H2A in mono-prenucleosomes, as there was a ratio of approximately 1.0:1.4 of wild-type H2A to Strep-H2A. This ratio is nearly identical to the theoretical expectation of 1.0:1.3 for an octamer (given the 3:1 ratio of wild-type H2A to Strep-tagged H2A prior to precipitation). These results therefore support the conclusion that a mono-prenucleosome comprises 80 bp DNA and a histone octamer.

We additionally tested the salt lability of mono-prenucleosomes relative to mononucleosomes. In these experiments, we prepared mono-prenucleosomes and mono-nucleosomes by salt dialysis (with 80 bp and 146 bp DNA fragments, respectively), adjusted the final NaCl concentrations to 0.1 M, 0.3 M, 0.8 M, or 2.0 M, and then subjected the samples to sucrose gradient sedimentation at the same salt concentrations (Fig. S2B). As a reference, mono-nucleosomes partially disassemble at 0.8 M NaCl, as seen with native chromatin (see, for example, Germond et al. 1976), and are completely disassembled at 2.0 M NaCl. In contrast, mono-prenucleosomes begin to dissemble at 0.3 M NaCl and are substantially disassembled at 0.8 M NaCl. Thus, consistent with the fewer histone-DNA contacts in prenucleosomes relative to nucleosomes, mono-prenucleosomes are more salt labile than canonical nucleosomes.

Mono-prenucleosomes can be converted into canonical nucleosomes by ACF

A key property of prenucleosomes is their ability to be converted into canonical nucleosomes by ACF (Torigoe et al. 2011). Therefore, we tested whether mono-prenucleosomes can be converted into canonical nucleosomes. To address this question, we formed poly-prenucleosomes by head-to-tail ligation of the 80 bp DNA in mono-prenucleosomes to free DNA. Next, we incubated the poly-prenucleosomes with ACF and ATP, and then digested the reaction products extensively with micrococcal nuclease (MNase), which converts nucleosome

arrays into core particles that contain approximately 147 bp DNA (Fig. 4A). This experiment revealed that ACF is able to convert poly-prenucleosomes into canonical nucleosomes, as assessed by the generation of the ~147 bp DNA species that is diagnostic of core particles. In the absence of ACF, we did not detect 147 bp DNA fragments upon digestion of the poly-prenucleosomes with MNase. Thus, the conversion of poly-prenucleosomes to polynucleosomes is dependent upon ACF. In addition, the ability of mono-prenucleosomes to be converted into canonical nucleosomes further supports the conclusion that mono-prenucleosomes contain a complete histone octamer.

In related experiments, we observed the conversion of mono-prenucleosomes to mononucleosomes by ligation of free DNA tails (85 bp) onto mono-prenucleosomes followed by the addition of ACF (Fig. 4B). As seen with the ligated poly-prenucleosomes (Fig. 4A) as well as with prenucleosomes formed by deposition of histones onto relaxed plasmid DNA (Torigoe et al. 2011), the conversion of prenucleosomes to canonical nucleosomes is dependent upon the ACF motor protein. These experiments, along with the results in Figs. S3A and S3B, further show that prenucleosomes formed with NAP1 or by salt dialysis can be converted into nucleosomes by ACF and that this process can occur with the 80 bp genomic DNA fragment or the central 80 bp of 601 DNA.

It is particularly notable that the ligation of free DNA to mono-prenucleosomes does not result in the spontaneous wrapping of the DNA around the histones to give a canonical nucleosome. We hypothesize that the histone octamer is slightly unfolded or expanded in prenucleosomes relative to nucleosomes, and that this alternate conformation of the histones in the prenucleosome does not enable facile wrapping of the DNA into a nucleosome. This postulated alternate conformation of the octamer in prenucleosomes could be due to charge repulsion between the histones that occurs in the absence of the extra histone-DNA contacts in canonical nucleosomes.

We also found that the Chd1 motor protein can be used in place of ACF for the conversion of ligated mono-prenucleosomes to nucleosomes (Fig. S3C). Hence, mono-

prenucleosomes can be converted to nucleosomes in a variety of different conditions. Most importantly, these experiments reveal that mono-prenucleosomes are functionally active as precursors to canonical nucleosomes.

MNase analysis indicates that prenucleosomes contain approximately 80 bp DNA

To complement the results from the psoralen crosslinking and electron microscopy experiments (Fig. 1), we used the mono-prenucleosome system to re-examine the length of DNA that is closely associated with prenucleosomes. For these experiments, we employed MNase as a probe of histone-DNA interactions. In our studies of the ACF-mediated conversion of prenucleosomes to nucleosomes (Fig. 4), we observed that MNase digestion of prenucleosomes with ligated free DNA (in the absence of ACF) yields a set of bands of approximately 80 bp. We mapped the ends of these MNase digestion products by primer extension analysis and found that the majority of the DNA fragments ranged from about 78 to 85 bp in length and correlated with the central 80 bp 601 DNA that was used in the assembly of the mono-prenucleosomes (Fig. 5). The boundaries of MNase digestion of prenucleosomes are not as distinct as those seen with MNase digestion of canonical nucleosomes. Nevertheless, these results provide independent confirmation of the estimates of 70-80 bp of DNA per prenucleosome based on electron microscopy of prenucleosomes in relaxed plasmid DNA (Fig. 1). Collectively, these results indicate that prenucleosomes are closely associated with approximately 80 bp of DNA.

We also examined whether the DNA in a prenucleosome is accessible to restriction enzymes. To address this question, we assembled mono-prenucleosomes onto a variant of the 80 bp genomic DNA fragment that contains an EcoRV site (center of restriction site is 25/55 bp from the DNA ends) and an XhoI site (center of site is 46/34 bp from the ends). The addition of EcoRV or XhoI with mono-prenucleosomes versus naked DNA controls revealed that the packaging of DNA into mono-prenucleosomes blocks the access of the DNA to restriction

enzymes (Fig. S4), as seen with canonical nucleosomes. This restriction enzyme accessibility assay could be useful in the analysis of the properties of prenucleosomes.

The central region of the DNA in a mono-prenucleosome is located at approximately the same position as the analogous stretch of DNA in a core particle

We then sought to determine the location of the 80 bp DNA in the mono-prenucleosome. To this end, we employed the histone-directed DNA cleavage method of Flaus et al. (1996) with the use of N-(1,10-phenanthrolin-5-yl)iodoacetamide (OP) as the histone-modifying reagent (Brogaard et al. 2012; Henikoff et al. 2014). In these experiments, we used wild-type core histones as well as histone octamers containing the H4S47C or H2BT87C mutant histones. In particular, it should be noted that H4S47C in a nucleosome is located near the dyad (Flaus et al. 1996). Alkylation of the cysteine sulfhydryl group by OP results in a covalent linkage between an o-phenanthroline moiety and the cysteine residue. In the presence of Cu(II) and hydrogen peroxide, this o-phenanthroline group mediates the generation of hydroxyl radicals that cleave the nearby DNA.

We thus alkylated wild-type and mutant (H4S47C or H2BT87C) histones with OP, reconstituted mono-prenucleosomes with the modified histones and the central 80 bp of 601 DNA, and then examined the cleavage of DNA upon addition of Cu(II) and hydrogen peroxide. These experiments revealed distinct cleavage sites near the middle of the 601 DNA sequence with the modified H4S47C histones, but not with the wild-type or the H2BT87C histones (Fig. 6). The DNA cleavage was also dependent upon the addition of Cu(II). Strikingly, with the H4S47C histones, the sites of DNA cleavage of the central 80 bp 601 fragment in mono-prenucleosomes are identical to those seen in canonical nucleosomes with the full 147 bp 601 DNA fragment (Henikoff et al. 2014). That is, the central 80 bp of 601 sequence in the mono-prenucleosome is located at the analogous position as the same DNA segment in a canonical nucleosome with the full 147 bp 601 DNA. We also observed a related DNA cleavage pattern of the 80 bp genomic DNA with the H4S47C histones (Fig. S5), but the results were less distinct, possibly

due to some heterogeneity in the interaction of the 80 bp genomic DNA to prenucleosomes relative to that of the well-positioned central 80 bp of 601 DNA. Hence, these findings indicate that the central region of the DNA in a mono-prenucleosome is located at approximately the same position as the analogous stretch of DNA in a core particle.

It is also relevant to note that the H2BT87C residue, which is located at the opposite side of the dyad in a canonical nucleosome (see, for example: Ferreira et al. 2007), was included as a probe in case the prenucleosomal DNA were located asymmetrically on the histone octamer. With its symmetric location, the prenucleosomal DNA would be cleaved by the OP-modified H2BT87C residue about 4-6 nt from the end (if the prenucleosome had the same histone-DNA contacts as a nucleosome) and yield small fragments that could not be clearly resolved. Thus, the absence of distinct cleavage sites with H2BT87C is not definitive but is consistent with the proposed central location of the DNA in the prenucleosome.

p300 specifically acetylates H3K56 in prenucleosomes relative to nucleosomes

We further investigated the properties of prenucleosomes by subjecting prenucleosomes and nucleosomes to acetylation by purified p300 and then analyzing the resulting histones by mass spectrometry. Among the possible candidates for prenucleosome-specific acetylation by p300, H3K56 is the only amino acid residue that was found to exhibit this property (Fig. 7A). Acetylation of H3K56 by p300 occurs with prenucleosomes but not with NAP1-histone complexes or with nucleosomes. In addition, the acetylation at H3K56 was confirmed by the parallel analysis of H3K56A, with which acetylation was not detected.

In metazoans, H3K56 is acetylated by CBP/p300 proteins (Das et al. 2009). H3K56 is located at the DNA entry and exit points of the nucleosome (see, for example: Masumoto et al. 2005; Xu et al. 2005). Hence, the greater accessibility of p300 to H3K56 in prenucleosomes relative to nucleosomes is consistent with the location of prenucleosomal DNA in the region that corresponds to the central 80 bp of the nucleosome (Fig. 6).

H3K56ac has been found to be involved in chromatin assembly during DNA replication and repair (see, for example: Masumoto et al. 2005; Han et al. 2007; Li et al. 2008; Chen et al. 2008). In addition, genome-wide chromatin immunoprecipitation experiments in yeast, *Drosophila*, and human cells have shown that H3K56ac is highly enriched at active promoters as well as at enhancers (see, for example: Lo et al. 2011; Venkatesh et al. 2012; Skalska et al. 2015). Moreover, in *Drosophila*, the increase in H3K56 acetylation at promoters and enhancers by Notch activation was found to occur rapidly by a mechanism that requires CBP acetyltransferase activity but not transcriptional elongation (Skalska et al. 2015). These findings suggest that pre-existing H3K56 can be acetylated by CBP.

Thus, the specific acetylation of H3K56 in prenucleosomes relative to nucleosomes provides another link between the properties of prenucleosomes and dynamic chromatin in cells. It is also possible that presence of H3K56ac at promoters and enhancers may reflect the occurrence of prenucleosomes or prenucleosome-like particles. In the future, it should be interesting and informative to examine the relation between H3K56 acetylation and prenucleosome function in greater detail.

Discussion

The prenucleosome is a stable alternate conformational isomer of the nucleosome

The prenucleosome was initially identified as non-nucleosomal histone-DNA complex that is a precursor to the nucleosome in the assembly of chromatin in vitro (Torigoe et al. 2011). However, the ability to study prenucleosomes was limited by the heterogeneity of the prenucleosome samples that were assembled onto plasmid DNA templates. Hence, we lacked a fundamental understanding of the composition, structure, and organization of prenucleosomes.

In this study, we observed by psoralen crosslinking and electron microscopy that prenucleosomes appear to be associated with about 70-80 bp of DNA (Fig. 1). This finding led to the development of the mono-prenucleosome system that involves the assembly of monomeric prenucleosomes from the four core histones and an 80 bp DNA fragment (Fig. 2). Prenucleosomes contain a histone octamer and are distinct from species such as tetrasomes or hexasomes that contain less than a complete octamer (Figs. 2 and 3). Moreover, mono-tetrasomes can be converted into mono-prenucleosomes with no apparent accumulation of stable hexasome species (Fig. 2D). It is particularly notable that mono-prenucleosomes can be formed by the deposition of histones by NAP1 or dNLP as well as by salt dialysis (Fig. 2C). Importantly, mono-prenucleosomes are functionally active, as they can be ligated to free (naked) DNA and then converted into canonical nucleosomes by a motor protein such as ACF or Chd1 (Figs. 4 and S3).

By using histone-directed DNA cleavage methodology (Flaus et al. 1996; Brogaard et al. 2012; Henikoff et al. 2014), we mapped the location of the 80 bp DNA relative to the histone octamer in mono-prenucleosomes (Figs. 6 and S5). These experiments revealed that the central region of the 80 bp DNA in a mono-prenucleosome is at the analogous location as the central region of the DNA near the dyad in a canonical nucleosome. We additionally mapped the ends of the DNA fragments generated by MNase digestion of prenucleosomes, and found

that the amount of DNA that is closely associated with prenucleosomes is approximately 80 bp (Fig. 5). This is similar to the prenucleosomal DNA length that was independently estimated by psoralen crosslinking and electron microscopy (Fig. 1). The partial wrapping of DNA relative to that in a nucleosome is likely to be responsible for the lack of DNA supercoiling by prenucleosomes as well as for the ability of p300 to acetylate H3K56 in prenucleosomes but not in canonical nucleosomes (Fig. 7A).

These findings indicate that the prenucleosome is a stable alternate conformational isomer of the nucleosome (Fig. 7B). Moreover, no other histone-DNA particle was observed to be formed as efficiently and rapidly as prenucleosomes in the presence of the four core histones. Because there are probably only a small number of stable alternate conformations of the nucleosome, prenucleosomes may share a common fundamental structure with native non-nucleosomal particles such as those present at active chromatin throughout the genome.

As briefly discussed above, it is interesting to note that mono-prenucleosomes that are ligated to free DNA do not spontaneously fold into canonical nucleosomes. The prenucleosomal histones appear to be in a different conformation than the histone octamer in a canonical nucleosome, possibly due to charge repulsion between the histones because of the reduced histone-DNA contacts in prenucleosomes relative to nucleosomes.

Based on the ability of prenucleosomes to be formed rapidly and then converted into canonical nucleosomes by a motor protein such as ACF or Chd1, we imagine that prenucleosomes are generated and assembled into nucleosomes during processes, such as DNA replication, transcription, and repair, in which nucleosomes are disrupted. For instance, prenucleosomes have the same properties as histone-DNA complexes (in which H2B and H3 can be detected) at DNA replication forks that resemble nucleosomes but are formed much more rapidly than canonical nucleosomes (see, for example: McKnight and Miller 1977; McKnight et al. 1978; Worcel et al. 1978). In addition, some factors might be able to convert canonical nucleosomes directly into prenucleosomes, but such activities have not yet been identified.

Prenucleosomes appear to be related to non-nucleosomal histone-DNA complexes at active promoters

In our psoralen crosslinking and electron microscopy analysis of prenucleosomes versus nucleosomes, we observed a striking similarity between the distributions of psoralen bubble sizes with prenucleosomes versus nucleosomes compared to those obtained with active versus repressed promoters in vivo in yeast (Fig. 1C). These findings suggest that the "nucleosome-depleted regions" (NDRs; also termed "nucleosome-free regions", or NFRs) that are located immediately upstream of the transcription start site of active genes contain prenucleosomes or prenucleosome-like particles (Fig. 7C).

In further support of this hypothesis, MPE-seq analyses in mouse embryonic stem cells revealed that subnucleosome-sized chromatin fragments (including those containing 50-100 bp DNA) are located specifically in the upstream promoter region of active genes (Ishii et al. 2015). Notably, these non-canonical chromatin particles contain histones H2A and H3 by ChIP-seq analysis. Moreover, the degree of enrichment of the subnucleosome-sized, histone-containing particles in the upstream promoter region correlates with the level of gene transcription, as assessed by RNA-seq (Ishii et al. 2015). Hence, these 50-100 bp sized, histone-containing particles that are present at active promoters have features that are similar to those of prenucleosomes.

In addition, the ability of prenucleosomes, but not nucleosomes, to be acetylated at H3K56 by p300 (Fig. 7A) may be responsible, at least in part, for the observed enrichment of H3K56ac at active promoters and enhancers (see, for example: Lo et al. 2011; Venkatesh et al. 2012; Skalska et al. 2015). p300 is associated with transcriptional enhancers (see, for example: Heintzman et al. 2007; Visel et al. 2009), and it is possible that the enrichment of H3K56ac at enhancers is due to p300-mediated acetylation of prenucleosomes. In promoter regions, the averaged peak of H3K56 acetylation has been observed to flank the NDR at about -250 bp or about +250 bp relative to the +1 transcription start site. The absence of an H3K56ac peak

precisely at the NDR could be due to the increased fragmentation of the sensitive DNA at the NDR (relative to the DNA in bulk chromatin) during the sonication of the chromatin. To clarify this issue, the generation of chromatin fragments for H3K56ac chromatin immunoprecipitation might optimally be performed with mild DNA cleaving reagents such as methidiumpropyl-EDTA-Fe(II) [MPE-Fe(II)] or low concentrations of micrococcal nuclease, as in Ishii et al. (2015).

Prenucleosomes may also be related to "fragile" nucleosomes, which are MNase-sensitive nucleosomes that have been seen in yeast promoters (see, for example: Weiner et al. 2010; Xi et al. 2011; Knight et al. 2014; Kubik et al. 2015). In addition, in HeLa (human) cells, salt-labile nucleosomes containing histones H2A.Z and H3.3 have been found at active promoters (Jin et al. 2009). Thus, the NDRs of active promoters appear to contain prenucleosomes or prenucleosome-related species (Fig. 7C).

Why might prenucleosomes or prenucleosome-like particles be present in the NDRs of active promoters? Because prenucleosomes interact with only about 80 bp of DNA, they would be more easily altered or disrupted than canonical nucleosomes. Also, if disrupted or displaced, prenucleosomes could be rapidly reassembled. In these respects, prenucleosomes appear to be compatible with the function of transcription factors. An alternate but related viewpoint is that prenucleosomes are intermediates in the dynamic process of nucleosome disassembly and reassembly at active promoters (Fig. 7D; also see, Brown et al. 2013). It is even possible that prenucleosomes enhance transcription, such as in the establishment of the optimal structure of the active promoter. This notion is supported by the observation that the intensities of the H2B and H3 ChIP signals associated with the subnucleosome-sized DNA fragments correlates with transcriptional activity as measured by RNA-seq (Ishii et al. 2015). In the future, it will be interesting and important to investigate the potential role of prenucleosomes or prenucleosome-like structures at active promoters.

Conclusion and perspective

Chromatin in the eukaryotic nucleus is multidimensional. There are covalent modifications of the histones, histone variants, ATP-driven chromatin remodeling factors, non-histone chromosomal proteins, and non-nucleosomal chromatin particles. Notably, each of these dimensions of chromatin affects gene expression. The prenucleosome is the only known stable alternate conformer of the nucleosome and the only distinct non-nucleosomal histone-DNA particle that has been observed to be rapidly and efficiently formed on DNA in the presence of the four core histones, as in the nucleus. [For instance, as seen in Figs. 2C and 2D, H3-H4 tetrasomes are inefficiently formed and are rapidly converted into prenucleosomes in the presence of H2A-H2B.] It thus seems likely that many non-nucleosomal particles in the cell are prenucleosomes or prenucleosome-related particles. An additional attractive feature of this hypothesis is the ability of prenucleosomes to be converted into nucleosomes by ATP-dependent motor proteins such as ACF or Chd1. Hence, in this model, there is a productive dynamic interconversion between prenucleosomes and nucleosomes (Fig. 7D). In the future, it is our hope that the new knowledge of non-nucleosomal components of chromatin will contribute to an integrated understanding of the dynamic structure and function of our genome.

Materials and methods

Reagents and methodology

DNA oligonucleotides were synthesized by Integrated DNA Technologies (San Diego, CA). The sequences of the oligonucleotides are given in Supplemental Table S1. *Drosophila melanogaster* NAP1 and ACF complex were synthesized in Sf9 cells by using baculovirus expression vectors and purified as described previously (Fyodorov and Kadonaga 2003). *D. melanogaster* dNLP was synthesized in *E. coli* and purified by the method of Ito et al. (1996). *D. melanogaster* Chd1 was synthesized in *E. coli* and purified as described (Torigoe et al. 2013). Native core histones were purified from *D. melanogaster* embryos that were collected from 0 to 12 hours after egg deposition (Fyodorov and Levenstein 2002). Recombinant *D. melanogaster* histones were synthesized in *E. coli* and purified by the method of Luger et al. (1999). Human p300 protein was purified and used as described in Kraus and Kadonaga (1998). All experiments were performed independently at least two times to ensure the reproducibility of the data.

Reconstitution of monomeric prenucleosomes (mono-prenucleosomes)

Mono-prenucleosomes were prepared either by histone chaperone-mediated deposition or by salt dialysis. In chaperone-mediated reconstitution reactions, the core histones were incubated with either NAP1 (at a 5:1 mass ratio of NAP1:core histones) or dNLP (at a 10:1 mass ratio of dNLP:core histones) on ice for 20 min in a volume of 10 µL in the following buffer: 10 mM K-HEPES (pH 7.6), 0.1 M KCl, 0.1 mM EDTA, 1 mM DTT, and 70 µg/mL bovine serum albumin. HEG buffer (8 µL) [25 mM K-HEPES (pH 7.6), 0.1 M KCl, 0.1 mM EDTA, and 10% (v/v) glycerol] was then added. Next, the preannealed DNA oligonucleotides (2 µL) [in 10 mM Tris-HCl (pH 7.5), 0.1 mM EDTA, 0.05 M NaCl] were added to the histone-chaperone mixture to give a final volume of 20 µL. The samples were mixed immediately by gentle vortexing, incubated for 30 s, and analyzed by native 5% polyacrylamide gel electrophoresis.

Salt dialysis reconstitution of mononucleosomes, mono-prenucleosomes, and mono-tetrasomes were performed by the method of Stein (1989). In a standard reaction, the DNA fragment (as indicated for each experiment) [50 pmol; 6 µL; in TE buffer: 10 mM Tris-HCl (pH 7.5), 1 mM EDTA] was combined with 140 µL of TE buffer containing 1.07 M NaCl and 0.011% (v/v) NP-40; then, core histones [50 pmol; 4 µL; in 10 mM K-HEPES (pH 7.6), 0.1 M KCl, 1 mM DTT, and 10% (v/v) glycerol] were added to give a final concentrations of 1.0 M NaCl and 0.01% (v/v) NP-40 in a total volume of 150 µL. The resulting histone-DNA mixture was subjected to dialysis at room temperature in a ThermoFisher Slide-A-Lyzer dialysis cassette (molecular weight cutoff of 3500 Daltons) for 2 h against TE containing 0.8 M NaCl, 1.5 h against TE containing 0.6 M NaCl, and 2 h against TE containing 0.05 M NaCl. The resulting products were analyzed by native 5% polyacrylamide gel electrophoresis. Mono-prenucleosomes that are reconstituted by salt dialysis are stable for at least a few weeks at 4˚C. For storage, prenucleosomes are dialyzed overnight at 4˚C against histone storage buffer [10 mM K-HEPES (pH 7.6), 0.1 mM EDTA, 0.1 M KCl, 10% (v/v) glycerol, and 1 mM DTT].

Ligation of mono-prenucleosomes to free DNA and assembly into canonical nucleosomes by ACF

Mono-prenucleosomes were ligated to free (naked) DNA by using methods similar to those employed for the ligation of nucleosomes to free DNA (Clark and Felsenfeld 1992; Stein et al. 2002). Typically, mono-prenucleosomes (85 pmol DNA with sticky ends) and the flanking DNA strands (85 pmol each; each with a single sticky end that is complementary to one end of the prenucleosomal DNA) were combined in 10 mM K-HEPES (pH 8.0), 1 mM EGTA, 1 mM DTT, 0.5 mM ATP, an ATP-regeneration system (3 mM phosphoenolpyruvate and 20 U/µL pyruvate kinase), 2.5 mM $MgCl_2$, 12.5 µg bovine serum albumin, and 3000 U of T4 DNA ligase (NEB) in a volume of 138 µL. HEG (82 µL) was added to give a final volume of 220 µL, and the ligation was carried out overnight at 16˚C. In the assembly of prenucleosomes into nucleosomes, the ligated prenucleosomes (20 pmol; 52 µL; directly from the ligation reaction) were combined with

a solution of 20 mM ATP and 33 mM $MgCl_2$ (5 µL), ACF (1.0 µL of 700 nM ACF to a final ACF concentration of 6 nM), and HEG buffer (17 µL) to a final volume of 70 µL. The reaction was carried out for 1.5 h at 27˚C. The samples were analyzed by MNase digestion as described in Torigoe et al. (2011).

Trimethylpsoralen crosslinking

Crosslinking was performed essentially as described (Sogo and Thoma 1989; Brown et al. 2015). The specific conditions are as follows. A 175 µL sample of chromatin assembly reaction (Torigoe et al. 2011; Fyodorov and Kadonaga 2003) was diluted with 125 µL of Dilution Buffer [15 mM K-HEPES (pH 7.6), 100 mM KCl, 5 mM $MgCl_2$, 0.1 mM EDTA, 6.6% (v/v) glycerol, 1% (w/v) polyvinyl alcohol (average MW 10,000), 1% (w/v) polyethylene glycol 8000, and 20 µg/mL bovine serum albumin] and transferred to a single well of a 24-well plate. The 24-well plate containing all samples was placed on an ice-water slurry and positioned 5 cm away from five 366 nm (15 W) UV bulbs in a Stratalinker 2400 (Stratagene). Seven rounds of the following steps were performed: (i) Addition of 15 µL of 400 µg/mL 4,5',8-trimethylpsoralen (Sigma) in 100% ethanol; (ii) Incubation in the dark for 5 min, on ice; (iii) Irradiation by UV for 5 min. Following crosslinking, 5 µL of 20 mg/mL of proteinase K and 20 µL of 10% (w/v) SDS were added, and the samples were incubated for 1 h at 55°C. DNA was extracted with phenol-chloroform and precipitated. DNA was resuspended, digested with EcoRI, purified by using a DNA Clean and Concentrator Kit (Zymo Research), and eluted from the column with 8 µL of TEN (30 mM tetraethylammonium chloride, 20 mM EDTA, 10 mM NaCl). Maximal crosslinking was verified with naked, relaxed DNA.

Sample preparation for electron microscopy

DNA (1-3 µL in TEN) was denatured in 70% (v/v) deionized formamide (Sigma) and 0.5 M glyoxal (Sigma) in a total volume of 13 µL for 30 min at 37°C. Samples were immediately placed on ice and diluted with 5 µL TEN. Benzalkonium chloride (Sigma) was added to 0.001%

(w/v) to facilitate spreading of the DNA. A 10 cm petri dish, with a mica ramp resting on the rim, was filled with distilled water. Graphite powder was lightly dusted on the surface of the water. A portion (5 µL) of the denatured DNA sample was run down the mica ramp and spread on top of the water, which pushed back the graphite dusting. DNA near the graphite border or mica ramp was picked up by using carbon-coated copper grids (Electron Microscopy Sciences), pre-treated with 30 µg/ml ethidium bromide. Grids were stained with 0.5 mM uranyl acetate, washed with 100% ethanol, and air-dried. Following staining, they were secured to a Rotary-Tilt Stage in a 208C High Vacuum Turbo Carbon Coater equipped with a Metal Evaporation Accessory (Cressington) and shadowed at an angle of 3° with Platinum:Palladium (80:20, Electron Microscopy Sciences) until a Thickness Monitor (MTM-10, Cressington) reported 100 nm of metal deposition on the sensor.

Electron microscopy

Images were taken on a JEOL 1230 electron microscope at 120 keV at 20,000X magnification, and were processed and analyzed in ImageJ. Chromatin assembly reactions were performed four separate times, and a total of 380 and 376 molecules were analyzed from chromatin assembly reactions without and with the addition of ACF, respectively.

Additional Materials and Methods are included in the Supplemental Material.

Acknowledgments

This work is dedicated to Professor E. Peter Geiduschek in recognition of his many fundamental and important contributions to molecular biology. We thank E. Peter Geiduschek, Russell F. Doolittle, Long Vo ngoc, and Yuan Wang for critical reading of the manuscript. We are grateful to Kristin Brogaard and Ji-Ping Wang for their advice on the use of N-(1,10-phenanthrolin-5-yl)iodoacetamide. We also thank Arnold Stein for his advice on the ligation of mono-prenucleosomes to free DNA. J.T.K. is the Amylin Chair in the Life Sciences. This work was supported by grants from the NSF to H.B. (1243957) and from the NIGMS/NIH to J.T.K. (GM058272).

References

Arimura Y, Tachiwana H, Oda T, Sato M, Kurumizaka H. 2012. Structural analysis of the hexasome, lacking one histone H2A/H2B dimer from the conventional nucleosome. *Biochemistry* **51**: 3302-3309.

Bouazoune K, Kingston RE. 2013. Assembly, remodelled. *eLife* **2**: e01270.

Brogaard K, Xi L, Wang JP, Widom J. 2012. A map of nucleosome positions in yeast at base-pair resolution. *Nature* **486**: 496-501.

Brown CR, Mao C, Falkovskaia E, Jurica MS, Boeger H. 2013. Linking stochastic fluctuations in chromatin structure and gene expression. *PLOS Biol* **11**: e1001621.

Brown CR, Eskin JA, Hamperl S, Griesenbeck J, Jurica MS, Boeger H. 2015. Chromatin structure analysis of single gene molecules by psoralen cross-linking and electron microscopy. *Methods Mol Biol* **1228**: 93-121.

Chen CC, Carson JJ, Feser J, Tamburini B, Zabaronick S, Linger J, Tyler JK. 2008. Acetylated lysine 56 on histone H3 drives chromatin assembly after repair and signals for the completion of repair. *Cell* **134**: 231-243.

Clark DJ, Felsenfeld G. 1992. A nucleosome core is transferred out of the path of a transcribing polymerase. *Cell* **71**: 11-22.

Das C, Lucia MS, Hansen KC, Tyler JK. 2009. CBP/p300-mediated acetylation of histone H3 on lysine 56. *Nature* **459**: 113-117.

Ferreira H, Somers J, Webster R, Flaus A, Owen-Hughes T. 2007. Histone tails and the H3 alphaN helix regulate nucleosome mobility and stability. *Mol Cell Biol* **27**: 4037-4048.

Flaus A, Luger K, Tan S, Richmond TJ. 1996. Mapping nucleosome position at single base-pair resolution by using site-directed hydroxyl radicals. *Proc Natl Acad Sci USA* **93**: 1370-1375.

Fyodorov DV, Kadonaga JT. 2003. Chromatin assembly in vitro with purified recombinant ACF and NAP-1. *Methods Enzymol* **371**: 499-515.

Fyodorov DV, Levenstein ME. 2002. Chromatin assembly using *Drosophila* systems. *Curr. Protoc Mol Biol* **21**: 21.7.1-21.7.27.

Germond JE, Bellard M, Oudet P, Chambon P. 1976. Stability of nucleosomes in native and reconstituted chromatins. *Nucleic Acids Res* **3**: 3173-3192.

Han J, Zhou H, Horazdovsky B, Zhang K, Xu RM, Zhang Z. 2007. Rtt109 acetylates histone H3 lysine 56 and functions in DNA replication. *Science* **315**: 653-655.

Hanson CV, Shen CK, Hearst JE. 1976. Cross-linking of DNA in situ as a probe for chromatin structure. *Science* **193**: 62-64.

Heintzman ND, Stuart RK, Hon G, Fu Y, Ching CW, Hawkins RD, Barrera LO, Van Calcar S, Qu C, Ching KA, Wang W, Weng Z, Green RD, Crawford GE, Ren B. 2007. Distinct and predictive chromatin signatures of transcriptional promoters and enhancers in the human genome. *Nat Genet* **39**: 311-318.

Henikoff S, Ramachandran S, Krassovsky K, Bryson TD, Codomo CA, Brogaard K, Widom J, Wang JP, Henikoff JG. 2014. The budding yeast Centromere DNA Element II wraps a stable Cse4 hemisome in either orientation in vivo. *eLife* **3**: e01861.

Ishii H, Kadonaga JT, Ren B. 2015. MPE-seq, a new method for the genome-wide analysis of chromatin structure. *Proc Natl Acad Sci USA* **112**: E3457-3465.

Ito T, Tyler JK, Bulger M, Kobayashi R, Kadonaga JT. 1996. ATP-facilitated chromatin assembly with a nucleoplasmin-like protein from *Drosophila melanogaster*. *J Biol Chem* **271**: 25041-25048.

Jackson V, Chalkley R. 1981. A new method for the isolation of replicative chromatin: selective deposition of histone on both new and old DNA. *Cell* **23**: 121-134.

Jin C, Zang C, Wei G, Cui K, Peng W, Zhao K, Felsenfeld G. 2009. H3.3/H2A.Z double variant-containing nucleosomes mark 'nucleosome-free regions' of active promoters and other regulatory regions. *Nat Genet* **41**: 941-945.

Klempnauer KH, Fanning E, Otto B, Knippers R. 1980. Maturation of newly replicated chromatin of simian virus 40 and its host cell. *J Mol Biol* **136**: 359-374.

Knight B, Kubik S, Ghosh B, Bruzzone MJ, Geertz M, Martin V, Dénervaud N, Jacquet P, Ozkan B, Rougemont J, Maerkl SJ, Naef F, Shore D. 2014. Two distinct promoter architectures centered on dynamic nucleosomes control ribosomal protein gene transcription. *Genes Dev* **28**: 1695-1709.

Kraus WL, Kadonaga JT. 1998. p300 and estrogen receptor cooperatively activate transcription via differential enhancement of initiation and reinitiation. *Genes Dev.* **12**: 331-342

Kubic S, Bruzzone MJ, Jacquet P, Falcone JL, Rougemont J, Shore D. 2015. Nucleosome stability distinguishes two different promoter types at all protein-coding genes in yeast. *Mol Cell* **60**: 422-434.

Levy A, Jakob KM. 1978. Nascent DNA in nucleosome-like structures from chromatin. *Cell* **14**: 259-267.

Li Q, Zhou H, Wurtele H, Davies B, Horazdovsky B, Verreault A, Zhang Z. 2008. Acetylation of histone H3 lysine 56 regulates replication-coupled nucleosome assembly. *Cell* **134**: 244-255.

Lo KA, Bauchmann MK, Baumann AP, Donahue CJ, Thiede MA, Hayes LS, des Etages SA, Fraenkel E. 2011. Genome-wide profiling of H3K56 acetylation and transcription factor binding sites in human adipocytes. *PLoS One* **6**: e19778.

Lowary PT, Widom J. 1998. New DNA sequence rules for high affinity binding to histone octamer and sequence-directed nucleosome positioning. *J Mol Biol* **276**: 19-42.

Luger K, Rechsteiner TJ, Richmond TJ. 1999. Expression and purification of recombinant histones and nucleosome reconstitution. *Methods Mol Biol* **119**: 1- 16.

Masumoto H, Hawke D, Kobayashi R, Verreault A. 2005. A role for cell-cycle-regulated histone H3 lysine 56 acetylation in the DNA damage response. *Nature* **436**: 294-298.

McKnight SL, Miller OL Jr. 1977. Electron microscopic analysis of chromatin replication in the cellular blastoderm *Drosophila melanogaster* embryo. *Cell* **12**: 795-804.

McKnight SL, Bustin M, Miller OL Jr. 1978. Electron microscopic analysis of chromosome metabolism in the *Drosophila melanogaster* embryo. *Cold Spring Harbor Symp Quant Biol* **42**: 741-754.

Schlaeger EJ, Knippers R. 1979. DNA-histone interaction in the vicinity of replication points. *Nucleic Acids Res* **6**: 645-656.

Seale RL. 1975. Assembly of DNA and protein during replication in HeLa cells. *Nature* **255**: 247-249.

Seale RL. 1976. Studies on the mode of segregation of histone nu bodies during replication in HeLa cells. *Cell* **9**: 423-429.

Skalska L, Stojnic R, Li J, Fischer B, Cerda-Moya G, Sakai H, Tajbakhsh S, Russell S, Adryan B, Bray SJ. 2015. Chromatin signatures at Notch-regulated enhancers reveal large-scale changes in H3K56ac upon activation. *EMBO J* **34**: 1889-1904.

Sogo JM, Stahl H, Koller T, Knippers R. 1986. Structure of replicating simian virus 40 minichromosomes. The replication fork, core histone segregation and terminal structures. *J Mol Biol* **189**: 189-204.

Sogo JM, Thoma F. 1989. Electron microscopy of chromatin. *Meth Enzymol* **170**: 142-165.

Stein A. 1989. Reconstitution of chromatin from purified components. *Meth Enzymol* **170**: 585-603.

Stein A, Dalal Y, Fleury TJ. 2002. Circle ligation of in vitro assembled chromatin indicates a highly flexible structure. *Nucleic Acids Res* **20**: 5103-5109.

Torigoe SE, Urwin DL, Ishii H, Smith DE, Kadonaga JT. 2011. Identification of a rapidly formed nonnucleosomal histone-DNA intermediate that is converted into chromatin by ACF. *Mol Cell* **43**: 638-648.

Torigoe SE, Patel A, Khuong MT, Bowman GD, Kadonaga JT. 2013. ATP-dependent chromatin assembly is functionally distinct from chromatin remodeling. *eLife* **2**: e00863.

Venkatesh S, Smolle M, Li H, Gogol MM, Saint M, Kumar S, Natarajan K, Workman JL. 2012. Set2 methylation of histone H3 lysine 36 suppresses histone exchange on transcribed genes. *Nature* **489**: 452-455.

Visel A, Blow MJ, Li Z, Zhang T, Akiyama JA, Holt A, Plajzer-Frick I, Shoukry M, Wright C, Chen F, Afzal V, Ren B, Rubin EM, Pennacchio LA. 2009. ChIP-seq accurately predicts tissue-specific activity of enhancers. *Nature* **457**: 854-858.

Weiner A, Hughes A, Yassour M, Rando OJ, Friedman N. 2010. High-resolution nucleosome mapping reveals transcription-dependent promoter packaging. *Genome Res* **20**: 90–100.

Worcel A, Han S, Wong ML. 1978. Assembly of newly replication chromatin. *Cell* **15**: 969-977.

Xi Y, Yao J, Chen R, Li W, He X. 2011. Nucleosome fragility reveals novel functional states of chromatin and poises genes for activation. *Genome Res* **21**: 718–724.

Xu F, Zhang K, Grunstein M. 2005. Acetylation in histone H3 globular domain regulates gene expression in yeast. *Cell* **121**: 375-385.

Figure Legends

Figure 1. Psoralen crosslinking and electron microscopy analysis suggests that prenucleosomes associate with approximately 70-80 bp of DNA. (**A**) Analysis of prenucleosomes and nucleosomes by psoralen crosslinking followed by denaturing electron microscopy. Representative images are shown. The histone-free DNA is crosslinked by psoralen, and the resulting bubbles represent the locations of prenucleosomes and nucleosomes. (**B**) ACF-mediated conversion of prenucleosomes to canonical nucleosomes increases the size of psoralen bubbles from approximately 70-80 nt to approximately 140-150 nt. Prenucleosomes (−ACF) and nucleosomes (+ACF) were subjected to psoralen crosslinking and denaturing electron microscopy. Bubble sizes were measured in ImageJ and converted from nm to nucleotides. A total of 4,623 prenucleosome bubbles and 5,013 nucleosome bubbles were measured in four independent experiments. The plot displays the distribution of bubble sizes as the average ± standard deviation (N = 4) of 10 nt bins. The individual data points are placed at the center of the 10 nt bins. (**C**) Comparison of the psoralen bubble sizes observed in vitro and in vivo. The data from prenucleosomes and nucleosomes in vitro (B) and at the active versus repressed *PHO5* promoters in vivo in *S. cerevisiae* (Brown et al. 2013). The plot shows the distribution of bubble sizes as the average of 10 nt bins.

Figure 2. Rapid and efficient formation of monomeric prenucleosomes with 80 bp DNA fragments. (**A**) The NAP1-mediated formation of monomeric prenucleosomes (mono-prenucleosomes) with an 80 bp genomic DNA fragment occurs rapidly and requires all four core histones. Histone-NAP1 complexes were combined with an 80 bp DNA fragment (an 80 bp segment in the coding sequence of the *Drosophila melanogaster ISWI* gene; henceforth termed the "80 bp genomic DNA"). The samples were incubated at room temperature for 30 s and then subjected to native (nondenaturing) 5% polyacrylamide gel electrophoresis. The DNA was visualized by staining with ethidium bromide. One octamer equivalent of all four core histones

per DNA would be a 1:1 octamer:DNA ratio. Note that one octamer equivalent of H2A+H2B+H3+H4 has the same amount of H3 and H4 as one octamer equivalent of H3+H4. (**B**) Mono-prenucleosomes can be formed with the central 80 bp of the 601 nucleosome positioning sequence. Mono-prenucleosomes were formed and analyzed, as in (A), with all four core histones along with either the 80 bp genomic DNA or the central 80 bp of the 601 sequence. (**C**) Mono-prenucleosomes appear to be the thermodynamically most stable arrangement of the four core histones and 80 bp DNA at 50 mM NaCl. Mono-prenucleosomes were formed with the dNLP histone chaperone as well as by salt dialysis of the four core histones with the 80 bp genomic DNA fragment. For comparison, H3-H4 mono-tetrasomes were also generated in parallel by salt dialysis with H3-H4. The histones were used at an octamer equivalent:DNA ratio of 1.0. (**D**) Mono-tetrasomes can be converted into prenucleosomes by the addition of H2A-H2B. Mono-tetrasomes were formed by salt dialysis with the 80 bp genomic DNA, as in (C). Next, NAP1-H2A-H2B complexes were added, as indicated. The samples were incubated at room temperature for 30 s and then subjected to native 5% polyacrylamide gel electrophoresis. As a reference, a mono-prenucleosome formed by salt dialysis as in (C) was included ("Mono-prenuc").

Figure 3. Mono-prenucleosomes contain all four core histones and are distinct from hexasomes. (**A**) Sucrose gradient sedimentation analysis reveals that mono-prenucleosomes contain all four core histones. Mono-prenucleosomes were prepared either by NAP1-mediated deposition (left panels) or by salt dialysis (right panels), and then subjected to 10 to 30% (w/v, left to right) sucrose gradient sedimentation in a Beckman SW41 rotor (32,000 rpm, 4˚C, 18 h). The arrows indicate the direction of sedimentation. The presence of mono-prenucleosomes was detected by native polyacrylamide gel electrophoresis and ethidium bromide staining of the DNA (top panels). The protein composition was analyzed by SDS-polyacrylamide gel electrophoresis and silver staining (bottom panels). The top two fractions and the bottom fraction did not contain histones (see, for example, Fig. S2A) and are not included. The

sedimentation of the free core histones relative to prenucleosomal histones is shown in Fig. S2A. (**B**) Mono-prenucleosomes contain two copies of H2A and thus appear to contain a core histone octamer rather than hexamer. Mono-prenucleosomes were reconstituted with recombinant core histones onto the 80 bp genomic DNA by NAP1-mediated histone deposition. The H2A species were a combination of wild-type H2A and Strep-H2A at a 3:1 ratio of H2A:Strep-H2A. Prenucleosomes containing Strep-H2A were pulled down with Streptavidin-agarose, and then analyzed by western blot with antibodies against histone H2A. An H2A western blot and silver-stained SDS gel is also shown for the input samples. The western blots were detected and quantitated by using ^{32}P-labeled protein A.

Figure 4. Prenucleosomes can be converted into canonical nucleosomes by ACF. (**A**) ACF-dependent assembly of poly-prenucleosomes to polynucleosomes. Mono-prenucleosomes (prepared by salt dialysis with 80 bp genomic DNA containing two 5 nt overhangs) were ligated in a sequential head-to-tail fashion with free DNA (90 bp with two 5 nt overhangs) to give poly-prenucleosomes, as indicated in the diagram. The resulting poly-prenucleosomes were assembled into polynucleosomes with ACF and ATP. The formation of canonical nucleosomes was verified by micrococcal nuclease (MNase) digestion of the polynucleosomes into core particles, which contain approximately 147 bp DNA. (**B**) ACF-dependent assembly of mono-prenucleosomes to canonical nucleosomes. Mono-prenucleosomes (prepared by NAP1-mediated histone deposition with the central 80 bp of 601 DNA containing two 5 nt overhangs) were ligated to two free 80 bp DNA fragments (each containing a single 5 nt overhang) to give mono-prenucleosomes that are flanked by 85 bp DNA extensions, as illustrated in the diagram. The resulting mono-prenucleosomes were assembled into nucleosomes by ACF. The formation of canonical nucleosomes was assessed by MNase digestion into core particles that contain approximately 147 bp DNA. The 80 bp and 165 bp DNA fragments are incomplete ligation products.

Figure 5. MNase digestion analysis reveals that prenucleosomes are associated with approximately 80 bp of DNA. Mono-prenucleosomes were reconstituted by NAP1-mediated deposition onto the central 80 bp of the 601 DNA (with two 5 nt overhangs), and ligated to two free 80 bp DNA fragments (each containing a single 5 nt overhang) to give mono-prenucleosomes that are flanked by 85 bp DNA extensions, as indicated in the diagram. The samples were digested with MNase, and the 5' ends of the resulting DNA fragments were mapped by primer extension analysis. The 5' ends of the primers corresponded to the ends of the central 80 bp of the 601 sequences; thus, the majority of the MNase-digested fragments ranged in size from about 78 to 85 bp. The control lanes show the ends of the unligated (single white dots) and ligated (double white dots) DNA fragments prior to MNase digestion.

Figure 6. Mapping of the histone-DNA contacts in a mono-prenucleosome. Core histones containing the wild-type or the indicated mutant histones were modified with N-(1,10-phenanthrolin-5-yl)iodoacetamide (OP), which links an o-phenanthroline moiety onto the histones via alkylation of the thiol group on cysteine residues. The resulting derivatized histones were reconstituted by salt dialysis into mono-prenucleosomes with the central 80 bp of 601 DNA that is ^{32}P-labeled at the 5' end. The hydroxyl radical cleavage reactions were initiated by the addition of Cu(II), hydrogen peroxide, and mercaptopropionic acid. The cleavage products were purified and analyzed by electrophoresis on a 10% polyacrylamide-urea gel. The Maxam-Gilbert G+A ladder was used to identify the OP cleavage products, which are indicated at the right side of the autoradiogram. In a canonical nucleosome, H4S47C is located near the dyad.

Figure 7. The prenucleosome, a conformational isomer of the nucleosome. (**A**) p300 specifically acetylates histone H3K56 in prenucleosomes relative to nucleosomes. Chromatin assembly reactions with ACF (Torigoe et al. 2011; Fyodorov and Kadonaga 2003) were performed with relaxed circular plasmid DNA in the presence of acetyl-CoA. ATP (or UTP, as

the -ATP control), DNA, and p300 were included, as indicated. In addition, as a test for acetylation at H3K56, we performed parallel reactions with mutant histone H3K56A, which cannot be acetylated at H3 residue 56. The resulting samples were then subjected to western blot analysis with H3K56ac-specific antibodies (Millipore, cat. no. 07-677). As a reference, the blot was stripped and reprobed with anti-total H3 antibodies (Abcam, cat. no. AB1791). (**B**) Prenucleosomes comprise a core histone octamer and 80 bp DNA at a location that is analogous to that of the central 80 bp of the core particle. H3K56 is accessible to p300 in a prenucleosome but not in a nucleosome. Prenucleosomes can be converted into canonical nucleosomes by a motor protein such as ACF or Chd1. (**C**) Prenucleosomes or prenucleosome-related particles may be present in the upstream region of active promoters. (**D**) Model for the productive dynamic interconversion between prenucleosomes and nucleosomes. Prenucleosomes can be formed by the deposition of histones onto DNA and converted into nucleosomes by an ATP-driven motor protein such as ACF or Chd1. Nucleosomes can be disrupted by the action of enzymes such as polymerases as well as some ATP-driven chromatin remodeling factors. The resulting free histones are bound by the chaperones and then re-assembled into prenucleosomes. It is not known if a canonical nucleosome can be directly converted into a prenucleosome.

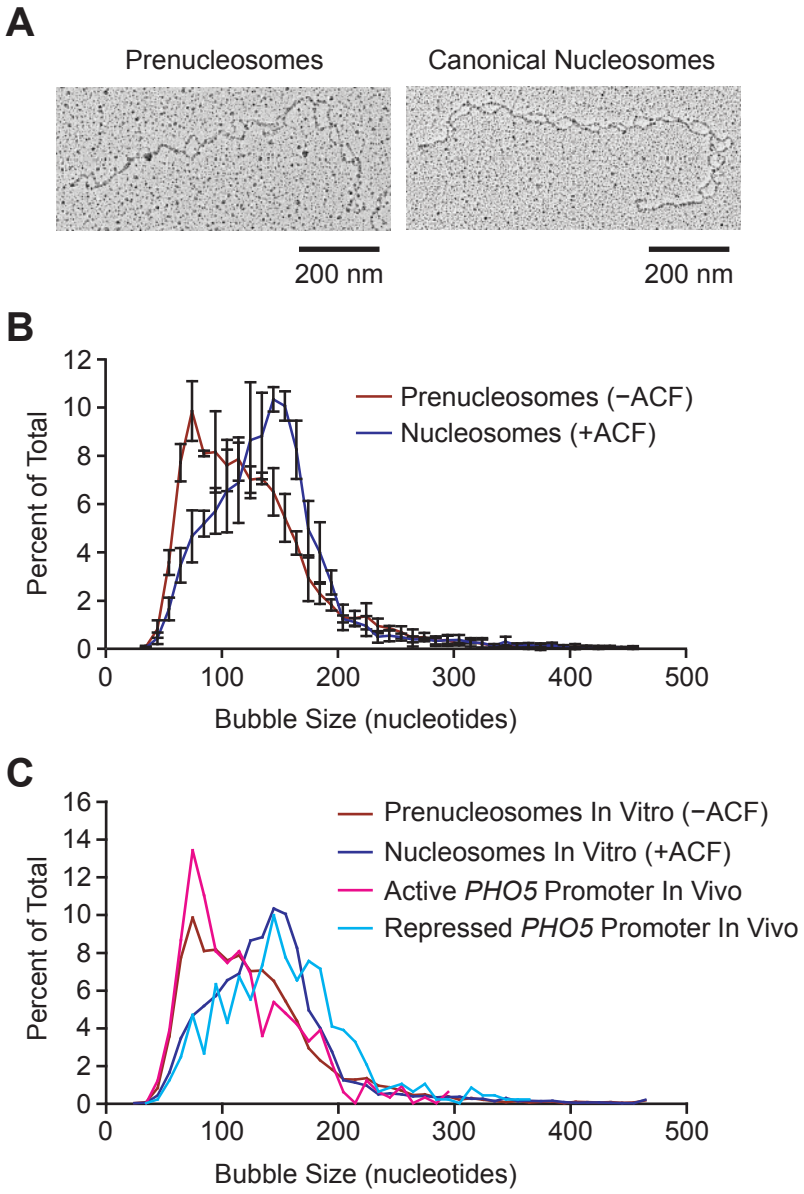
A
Prenucleosomes
Canonical Nucleosomes
200 nm
200 nm
B
Percent of Total
Prenucleosomes (−ACF)
Nucleosomes (+ACF)
Bubble Size (nucleotides)
C
Percent of Total
Prenucleosomes In Vitro (−ACF)
Nucleosomes In Vitro (+ACF)
Active PHO5 Promoter In Vivo
Repressed PHO5 Promoter In Vivo
Bubble Size (nucleotides)

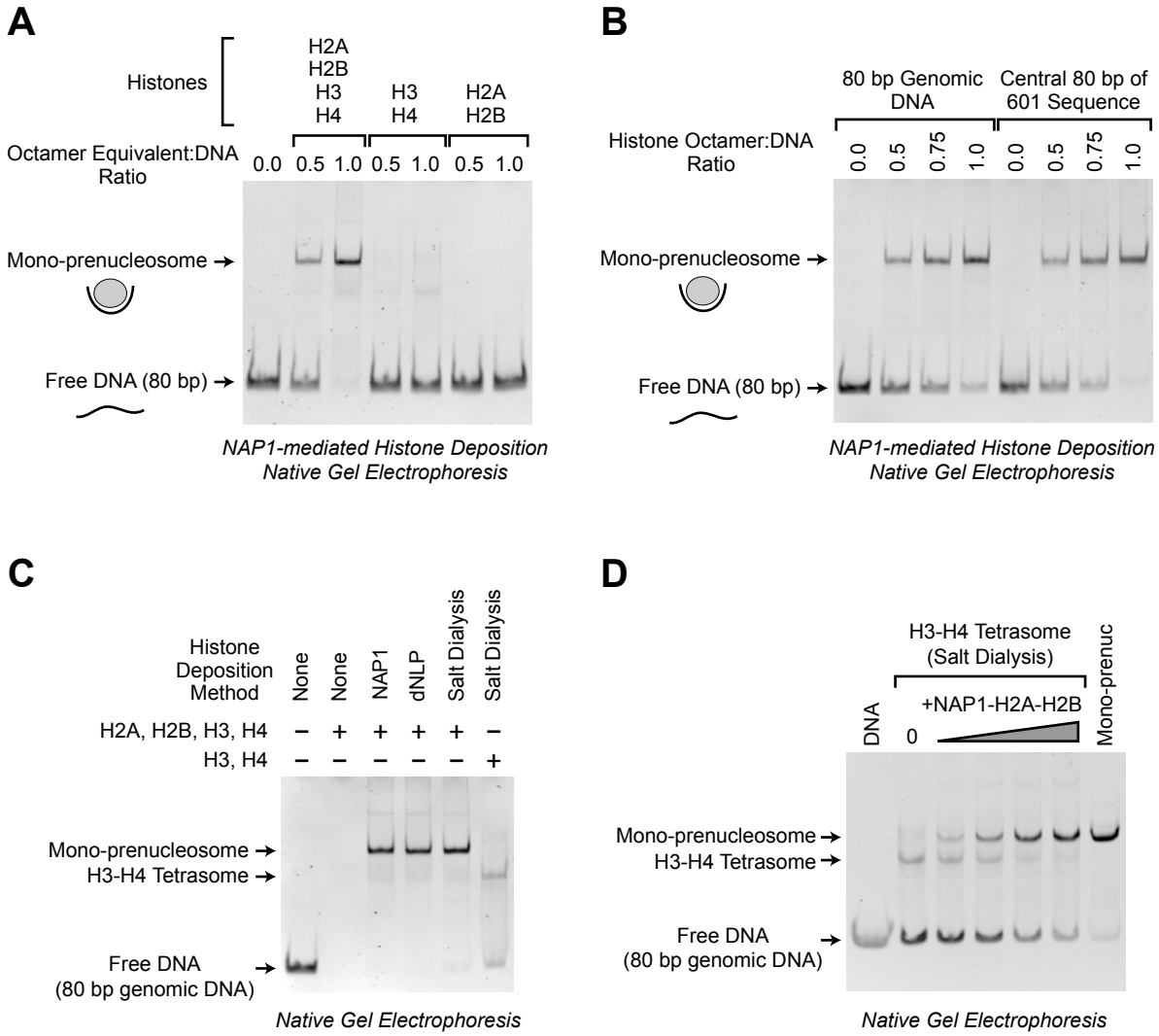
A
Histones
H2A
H2B
H3
H4
H3
H4
H2A
H2B
Octamer Equivalent:DNA Ratio
0.0 0.5 1.0 0.5 1.0 0.5 1.0
Mono-prenucleosome
Free DNA (80 bp)
NAP1-mediated Histone Deposition
Native Gel Electrophoresis
B
80 bp Genomic DNA
Central 80 bp of 601 Sequence
Histone Octamer:DNA Ratio
0.0 0.5 0.75 1.0 0.0 0.5 0.75 1.0
Mono-prenucleosome
Free DNA (80 bp)
NAP1-mediated Histone Deposition
Native Gel Electrophoresis
C
Histone Deposition Method
None
None
NAP1
dNLP
Salt Dialysis
Salt Dialysis
H2A, H2B, H3, H4 – + + + + –
H3, H4 – – – – – +
Mono-prenucleosome
H3-H4 Tetrasome
Free DNA
(80 bp genomic DNA)
Native Gel Electrophoresis
D
H3-H4 Tetrasome
(Salt Dialysis)
DNA
+NAP1-H2A-H2B
0
Mono-prenuc
Mono-prenucleosome
H3-H4 Tetrasome
Free DNA
(80 bp genomic DNA)
Native Gel Electrophoresis

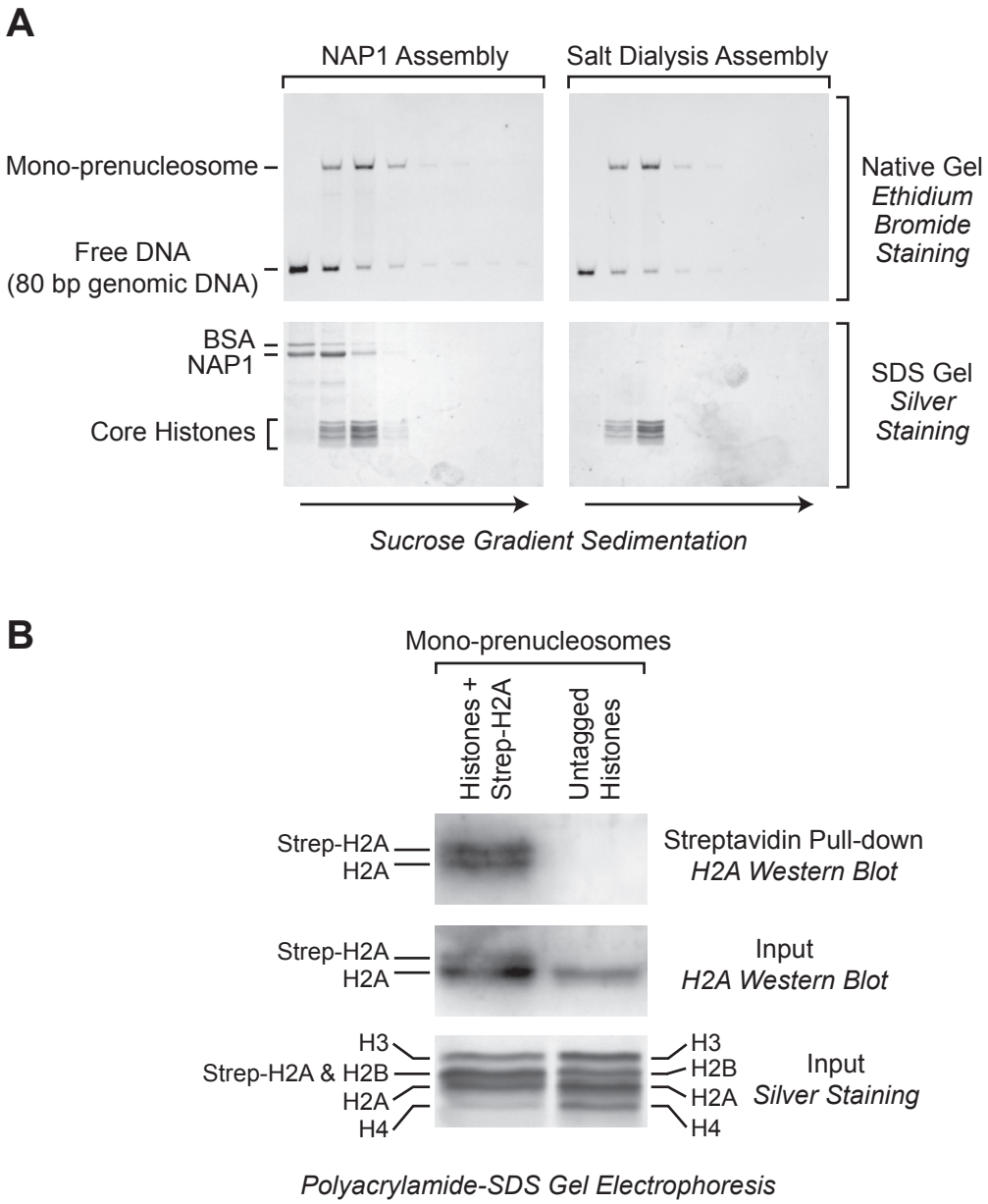
A
NAP1 Assembly
Salt Dialysis Assembly
Mono-prenucleosome
Free DNA
(80 bp genomic DNA)
Native Gel
Ethidium
Bromide
Staining
BSA
NAP1
Core Histones
SDS Gel
Silver
Staining
Sucrose Gradient Sedimentation
B
Mono-prenucleosomes
Histones +
Strep-H2A
Untagged
Histones
Strep-H2A
H2A
Streptavidin Pull-down
H2A Western Blot
Strep-H2A
H2A
Input
H2A Western Blot
H3
Strep-H2A & H2B
H2A
H4
H3
H2B
H2A
H4
Input
Silver Staining
Polyacrylamide-SDS Gel Electrophoresis

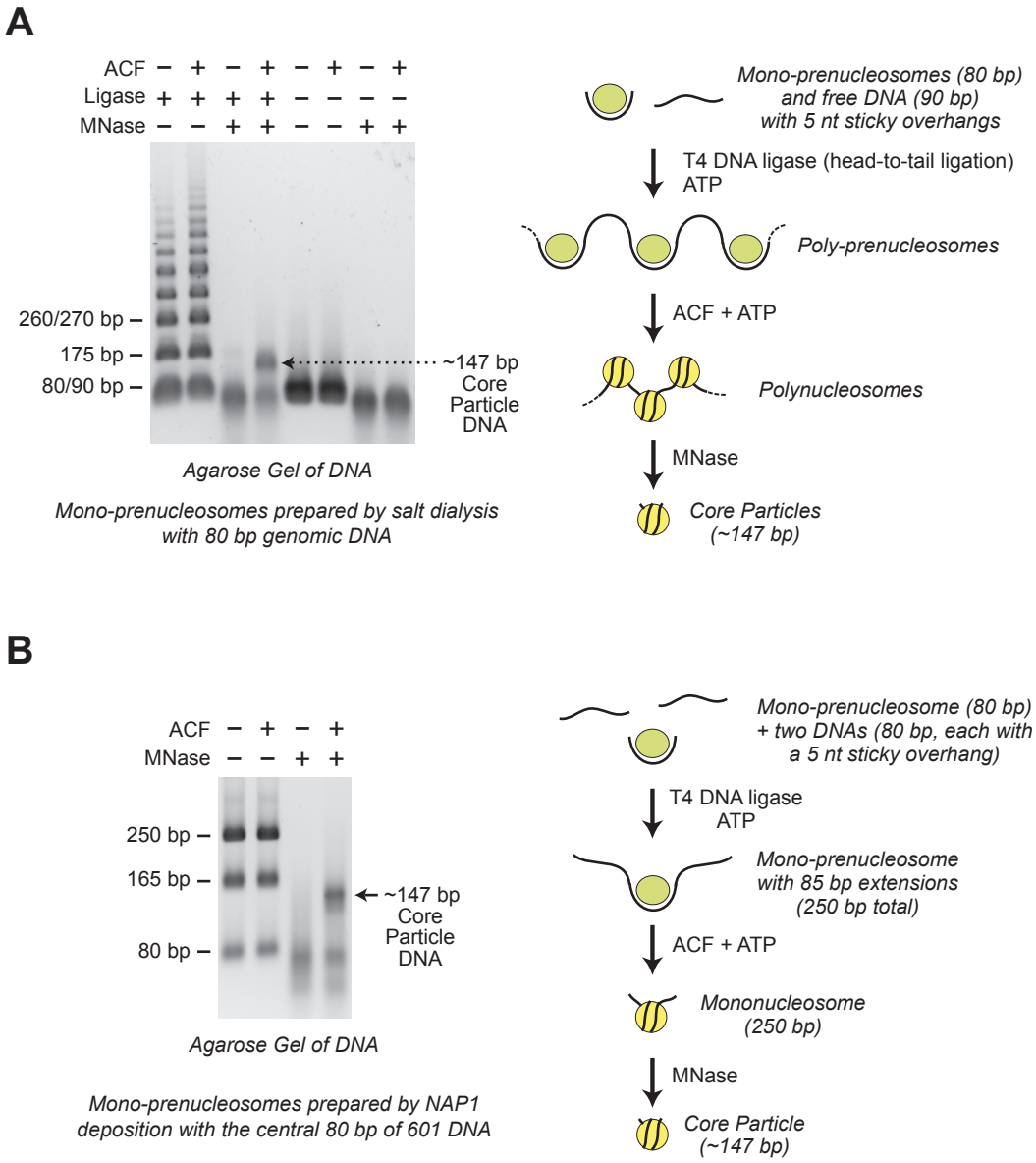
A
ACF − + − + − + − +
Ligase + + + + − − − −
MNase − − + + − − + +
260/270 bp
175 bp
80/90 bp
~147 bp Core Particle DNA
Agarose Gel of DNA
Mono-prenucleosomes prepared by salt dialysis with 80 bp genomic DNA
Mono-prenucleosomes (80 bp) and free DNA (90 bp) with 5 nt sticky overhangs
T4 DNA ligase (head-to-tail ligation)
ATP
Poly-prenucleosomes
ACF + ATP
Polynucleosomes
MNase
Core Particles (~147 bp)
B
ACF − + − +
MNase − − + +
250 bp
165 bp
80 bp
~147 bp Core Particle DNA
Agarose Gel of DNA
Mono-prenucleosomes prepared by NAP1 deposition with the central 80 bp of 601 DNA
Mono-prenucleosome (80 bp) + two DNAs (80 bp, each with a 5 nt sticky overhang)
T4 DNA ligase
ATP
Mono-prenucleosome with 85 bp extensions (250 bp total)
ACF + ATP
Mononucleosome (250 bp)
MNase
Core Particle (~147 bp)

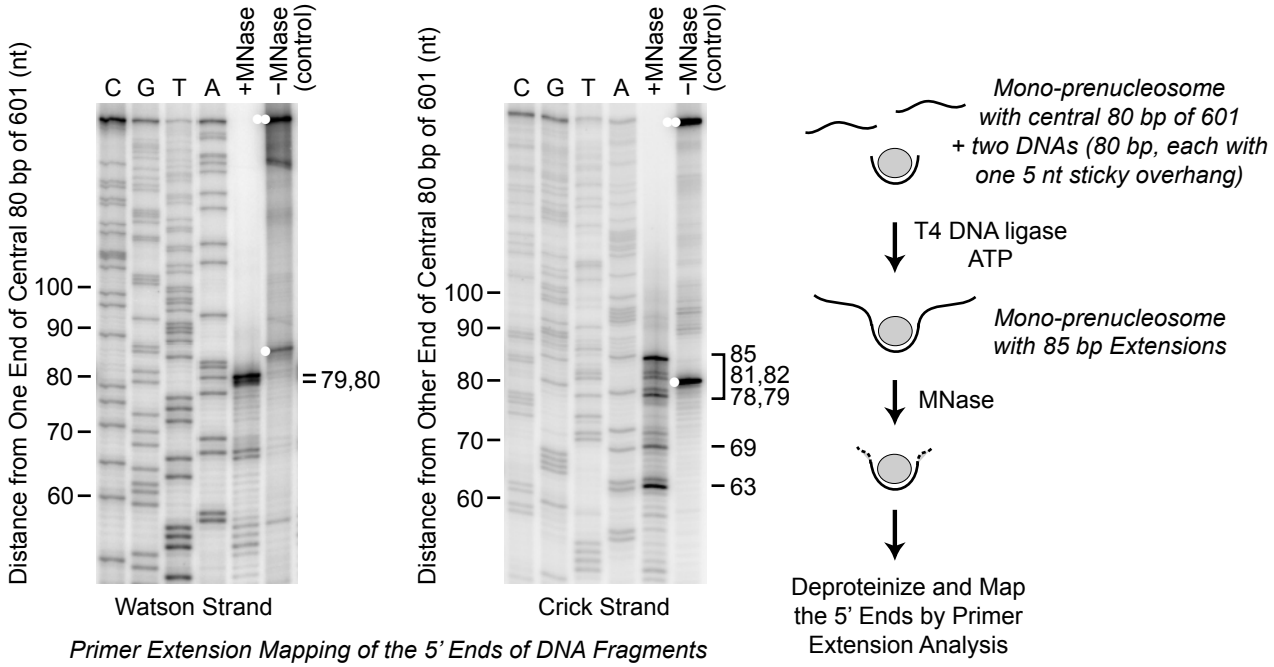

Primer Extension Mapping of the 5' Ends of DNA Fragments from MNase-digested Mono-prenucleosomes

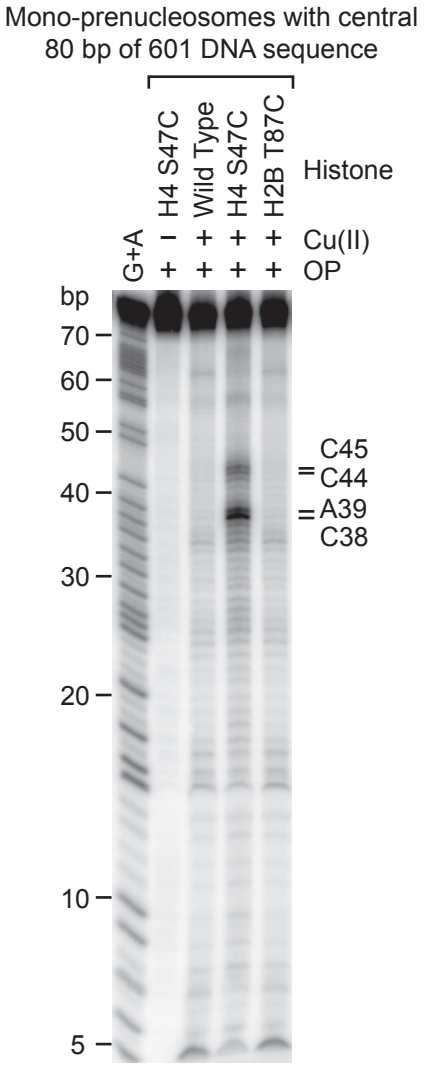

Cu(II)-catalyzed cleavage of DNA in the vicinity of histones linked to o-phenanthroline derivative (OP)

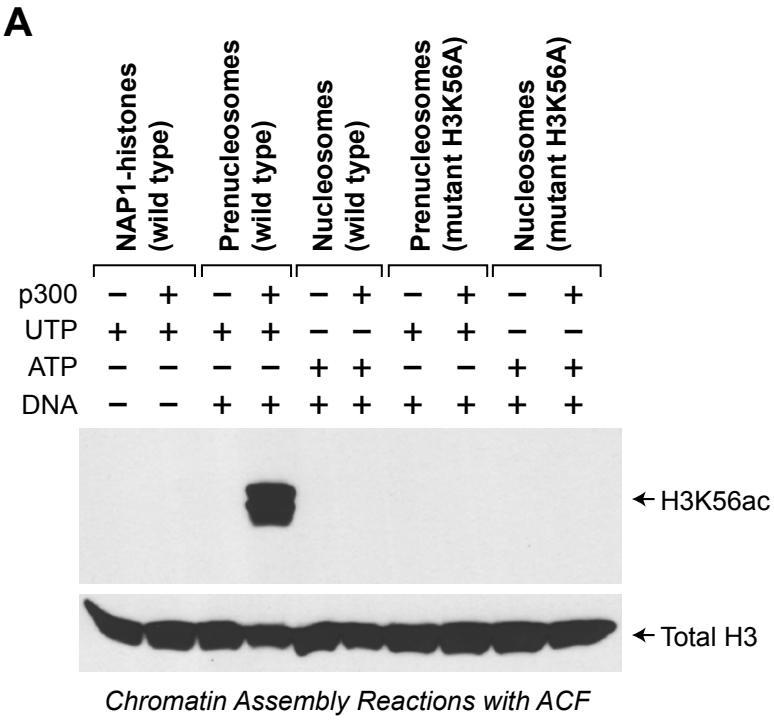
A
NAP1-histones (wild type)
Prenucleosomes (wild type)
Nucleosomes (wild type)
Prenucleosomes (mutant H3K56A)
Nucleosomes (mutant H3K56A)
p300 − + − + − + − + − +
UTP + + + + − − + + − −
ATP − − − − + + − − + +
DNA − − + + + + + + + +
H3K56ac
Total H3
Chromatin Assembly Reactions with ACF

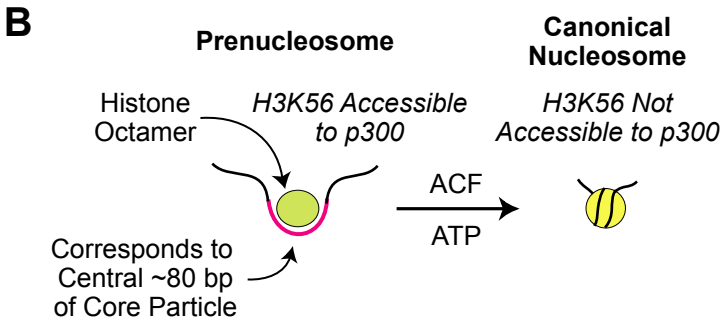
B
Prenucleosome
Canonical Nucleosome
Histone Octamer
H3K56 Accessible to p300
H3K56 Not Accessible to p300
ACF
ATP
Corresponds to Central ~80 bp of Core Particle

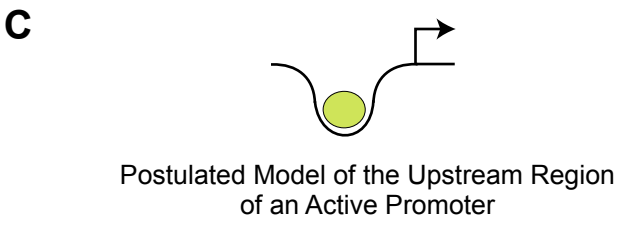
C
Postulated Model of the Upstream Region of an Active Promoter

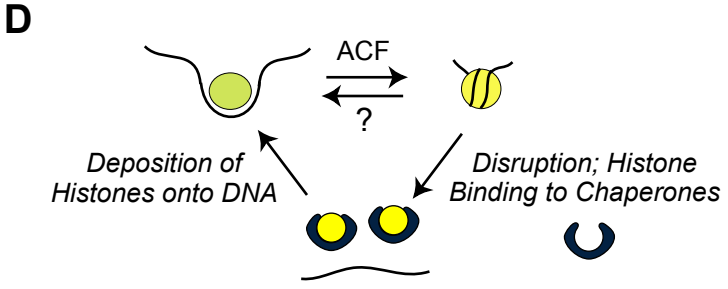
D
ACF
?
Deposition of Histones onto DNA
Disruption; Histone Binding to Chaperones

SUPPLEMENTAL MATERIAL

The Prenucleosome, a Stable Conformational Isomer of the Nucleosome

Jia Fei, Sharon E. Torigoe, Christopher R. Brown, Mai T. Khuong,
George A. Kassavetis, Hinrich Boeger, and James T. Kadonaga

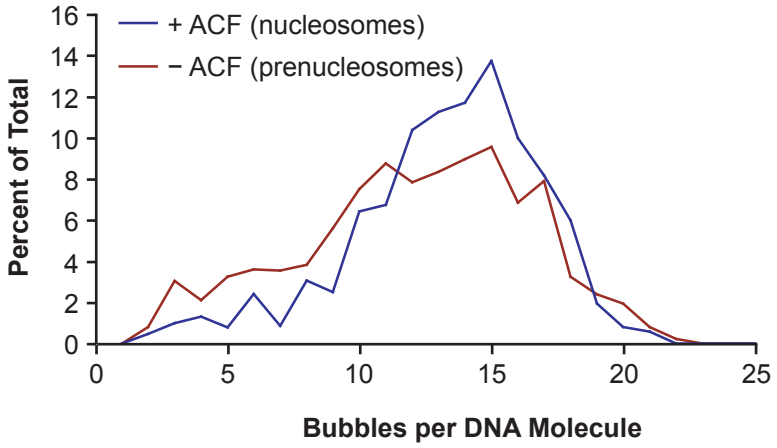

Supplemental Figure S1. The number of psoralen bubbles with prenucleosome templates (–ACF) is approximately the same as the number of bubbles with nucleosome templates (+ACF). The number of psoralen bubbles per plasmid DNA molecule was determined for the prenucleosome and nucleosome samples analyzed in Figure 1 of the main text. These data are based on the analysis of a total of 380 prenucleosome-containing molecules (–ACF) and 376 nucleosome-containing molecules (+ACF) in four independent experiments.

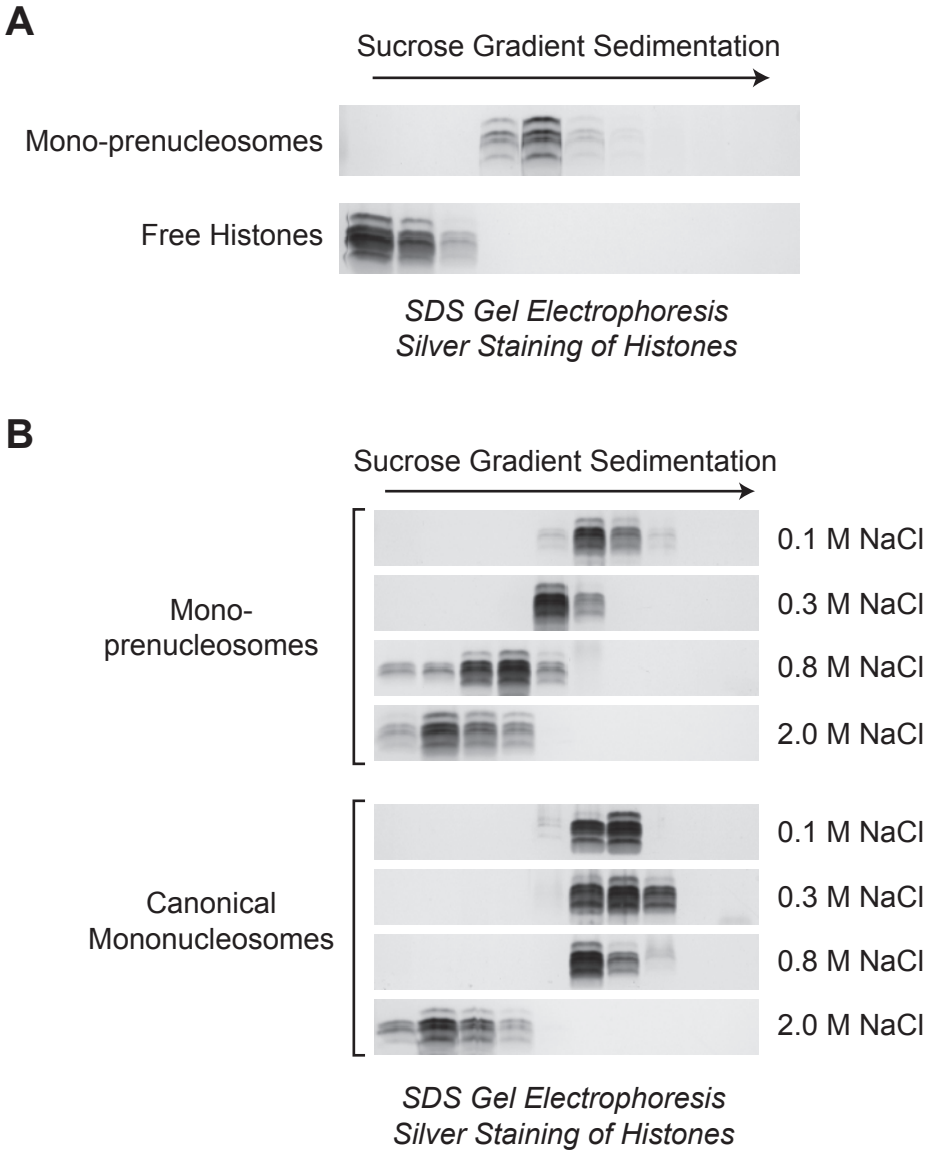

Supplemental Figure S2. Further characterization of mono-prenucleosomes by sucrose gradient sedimentation. (**A**) Mono-prenucleosomes sediment faster than free core histones. Mono-prenucleosomes were reconstituted with NAP1 and the 80 bp genomic DNA. The resulting prenucleosomes were then subjected to 10 to 30% (w/v, left to right) sucrose gradient sedimentation alongside the free core histones in a Beckman SW41 rotor (32,000 rpm, 4˚C, 18 h). The presence of the histones was determined by SDS-polyacrylamide gel electrophoresis and silver staining. (**B**) Mono-prenucleosomes are more salt labile than canonical nucleosomes. Mono-prenucleosomes were reconstituted by salt dialysis to a final concentration of 0.05 M NaCl with the 80 bp genomic DNA. Canonical mononucleosomes were reconstituted by salt dialysis to a final concentration of 0.05 M NaCl with the 146 bp 601 DNA. For each sample shown, the NaCl concentration was adjusted to the indicated amount by the addition of 5 M NaCl. Then, the samples were allowed to incubate at room temperature for 10 min and then subjected to 10 to 30% (w/v, left to right) sucrose gradient sedimentation at the same NaCl concentrations in a Beckman SW55 rotor (32,000 rpm, 4˚C, 17 h). The presence of the histones was determined by SDS-polyacrylamide gel electrophoresis and silver staining. The partial destabilization of the reconstituted canonical nucleosomes at 0.8 M NaCl is similar to that described previously with native nucleosomes (see, for example, Germond et al. 1976). The arrows indicate the direction of sedimentation.

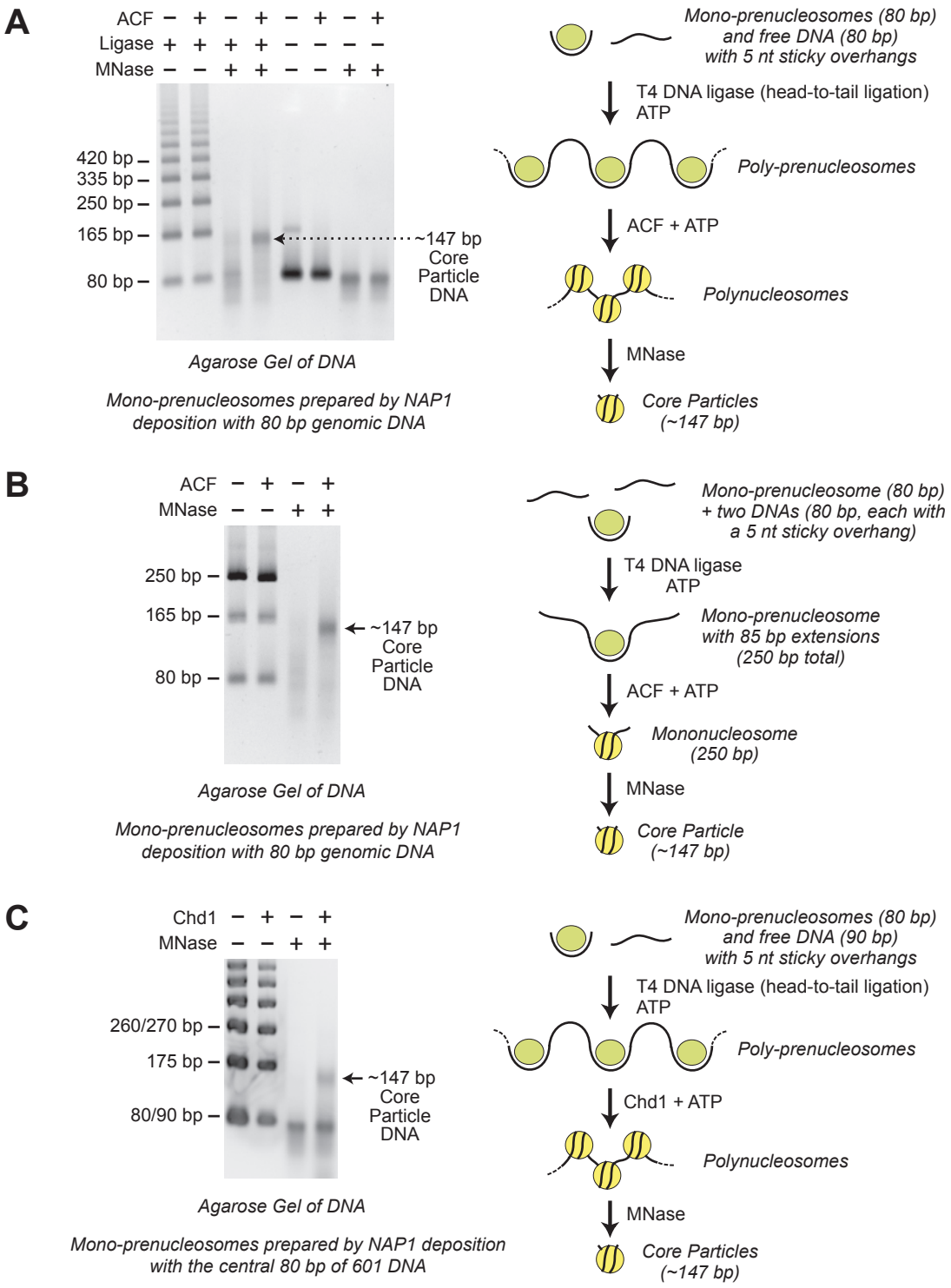

Supplemental Figure S3. Mono-prenucleosomes can be converted into canonical nucleosomes by ACF or Chd1. (**A**) ACF-catalyzed assembly of poly-prenucleosomes to polynucleosomes. Mono-prenucleosomes (prepared by NAP1-mediated deposition with 80 bp genomic DNA) were ligated to free DNA to give poly-prenucleosomes, and then assembled into polynucleosomes with ACF, as in Fig. 4A of the main text. (**B**) ACF-mediated assembly of mono-prenucleosomes to mononucleosomes. Mono-prenucleosomes (prepared by NAP1-mediated deposition with 80 bp genomic DNA) were ligated to free DNA and then assembled into mononucleosomes with ACF, as in Fig. 4B of the main text. (**C**) Chd1-catalyzed assembly of poly-prenucleosomes to polynucleosomes. Mono-prenucleosomes (prepared by NAP1-mediated deposition with the central 80 bp of 601 DNA) were ligated to free DNA to give poly-prenucleosomes, and then assembled into polynucleosomes with Chd1. The formation of canonical nucleosomes was verified by MNase digestion of the polynucleosomes into core particles (~147 bp DNA).

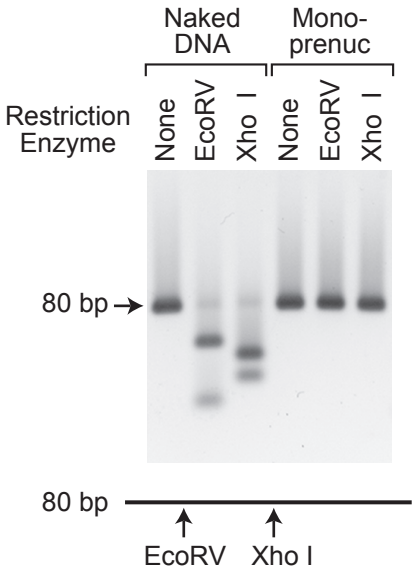

Supplemental Figure S4. Mono-prenucleosomes can block the access of restriction enzymes to DNA. Mono-prenucleosomes were reconstituted by NAP1 deposition with a variant of the 80 bp genomic DNA fragment that contains EcoRV and XhoI restriction sites. The center of the EcoRV restriction site is 25 and 55 bp from the ends of the 80 bp DNA fragment, whereas the center of the XhoI restriction site is 46 and 34 bp from the ends of the DNA. The mono-prenucleosomes were digested with the indicated enzymes along with the corresponding naked DNA fragments. The resulting DNA fragments were analyzed by agarose gel electrophoresis and staining with ethidium bromide.

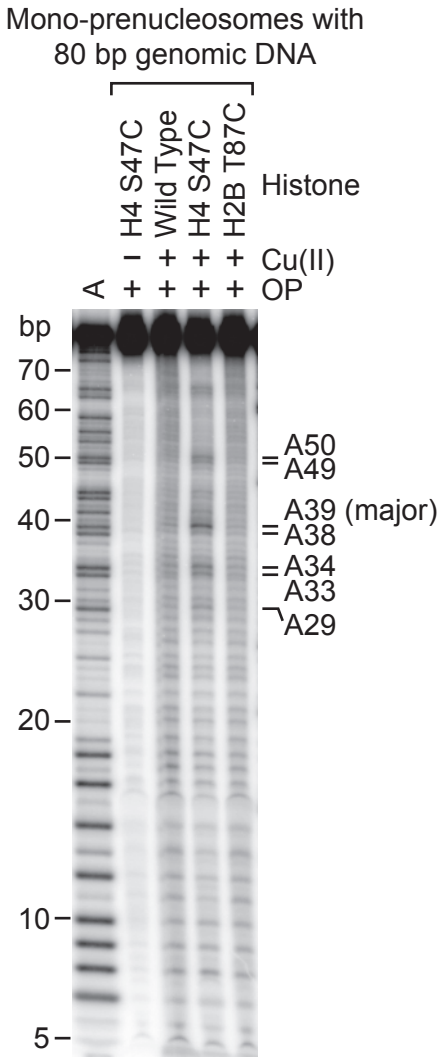

Cu(II)-catalyzed cleavage of DNA in the vicinity of histones linked to o-phenanthroline derivative (OP)

Supplemental Figure S5. Mapping of the histone-DNA contacts in mono-prenucleosomes assembled with 80 bp of genomic DNA. Core histones containing the wild-type or the indicated mutant histones were modified with N-(1,10-phenanthrolin-5-yl)iodoacetamide (OP), which links an o-phenanthroline moiety onto the histones via alkylation of the thiol group on cysteine residues. The resulting derivatized histones were reconstituted by salt dialysis into mono-prenucleosomes with 80 bp genomic DNA that is ^{32}P-labeled at the 5' end. The hydroxyl radical cleavage reactions were initiated by the addition of Cu(II), hydrogen peroxide, and mercaptopropionic acid. The cleavage products were purified and analyzed by electrophoresis on a 10% polyacrylamide-urea gel. An A-specific chemical sequencing reaction was used to identify the OP cleavage products, which are indicated at the right side of the autoradiogram. H4 S47C is located near the nucleosome dyad.

Supplemental Table S1. Oligonucleotides Used in this Study.

ISWI-80bp (Figs. 2, 3, S2, and S5)	Forward	ATG TCC AAA ACA GAT ACA GCT GCC GTG GAG GCA ACC GAA GAG AAC TCG AAC GAG ACG ACT TCA GAT GCG GCC ACC AGT TC
	Reverse	GAA CTG GTG GCC GCA TCT GAA GTC GTC TCG TTC GAG TTC TCT TCG GTT GCC TCC ACG GCA GCT GTA TCT GTT TTG GAC AT
601-80bp (Figs. 2B and 6)	Forward	TCG TAG ACA GCT CTA GCA CCG CTT AAA CGC ACG TAC GCG CTG TCC CCC GCG TTT TAA CCG CCA AGG GGA TTA CTC CCT AG
	Reverse	CTA GGG AGT AAT CCC CTT GGC GGT TAA AAC GCG GGG GAC AGC GCG TAC GTG CGT TTA AGC GGT GCT AGA GCT GTC TAC GA
ISWI-84bp-RE (Fig. S4)	Forward	CTA GAT TAC ATA TGT CCA AAA CAG AAG ATA TCG CCG TGG AGG CAA CCC TCG AGA ACT CGA ACG AGA CGC CAT GGG ATG CGG CCC
	Reverse	CCG GGG GCC GCA TCC CAT GGC GTC TCG TTC GAG TTC TCG AGG GTT GCC TCC ACG GCG ATA TCT TCT GTT TTG GAC ATA TGT AAT
ISWI-80-AN (Figs. 4A, S3A, and S3B)	Forward	/5Phos/CAT TCA TGT CCA AAA CAG ATA CAG CTG CCG TGG AGG CAA CCG AAG AGA ACT CGA ACG AGA CGA CTT CAG ATG CGG CCA CCA GTT CTT CCG
	Reverse	/5Phos/GAA CTG GTG GCC GCA TCT GAA GTC GTC TCG TTC GAG TTC TCT TCG GTT GCC TCC ACG GCA GCT GTA TCT GTT TTG GAC AT
ISWI-80-AN flank A (Figs. 4B, 5, and S3B)	Forward	/5Phos/ATC CGG TGA AAA GGA GGC TGA GTT CGA CAA CAA AAT CGA GGC TGA TCG CAG TAG GCG CTT TGA TTT CCT GCT AAA GCA GAC ATT C
	Reverse	GAA TGT CTG CTT TAG CAG GAA ATC AAA GCG CCT ACT GCG ATC AGC CTC GAT TTT GTT GTC GAA CTC AGC CTC CTT TTC ACC GGA TCG GAA
ISWI-80-AN flank B (Figs. 4B, 5, and S3B)	Forward	CGG AGA TAT TCA CCC ACT TCA TGA CTA ACA GCG CTA AGA GTC CCA CGA AGC CTA AGG GTA GAC CCA AGA AGA TCA AAG AC
	Reverse	/5Phos/GAA TGG TCT TTG ATC TTC TTG GGT CTA CCC TTA GGC TTC GTG GGA CTC TTA GCG CTG TTA GTC ATG AAG TGG GTG AAT ATC TCC G
ISWI-80bp-AN 90bp linker (Figs. 4A and S3C)	Forward	/5Phos/ATC CGG TGA AAA GGA GGC TGA GTT CGA CAA CAA AAT CGA GGC TGA TCG CAG TAG GCG CTT TGA TTT CCT GCT AAA GCA GAC GGA GAT ATT
	Reverse	/5Phos/GAA TGA ATA TCT CCG TCT GCT TTA GCA GGA AAT CAA AGC GCC TAC TGC GAT CAG CCT CGA TTT TGT TGT CGA ACT CAG CCT CCT TTT CAC CGG ATC GGA A
ISWI-80bp-AN 80bp linker (Fig. S3A)	Forward	/5Phos/ATC CGG TGA AAA GGA GGC TGA GTT CGA CAA CAA AAT CGA GGC TGA TCG CAG TAG GCG CTT TGA TTT CCT GCT AAA GCA GA
	Reverse	/5Phos/GAA TGT CTG CTT TAG CAG GAA ATC AAA GCG CCT ACT GCG ATC AGC CTC GAT TTT GTT GTC GAA CTC AGC CTC CTT TTC ACC GGA TCG GAA

601-80bp-AN (Figs. 4B, 5, and S3C)	Forward	/5Phos/CAT TCT CGT AGA CAG CTC TAG CAC CGC TTA AAC GCA CGT ACG CGC TGT CCC CCG CGT TTT AAC CGC CAA GGG GAT TAC TCC CTA GTT CCG
	Reverse	/5Phos/CTA GGG AGT AAT CCC CTT GGC GGT TAA AAC GCG GGG GAC AGC GCG TAC GTG CGT TTA AGC GGT GCT AGA GCT GTC TAC GA
Primers for Primer extension (Fig. 5)	Watson strand	TCG TAG ACA GCT CTA GCA CCG C
	Crick strand	CTA GGG AGT AAT CCC CTT GGC G

Supplemental Materials and Methods

Analysis of mono-prenucleosome composition by Strep-H2A pulldown

Mono-prenucleosomes were reconstituted with recombinant core histones onto the 80 bp genomic DNA by NAP1-mediated histone deposition. The core histones were either the wild-type histones, as a control, or a mixture of wild-type histones and Strep-H2A at a 3:1 ratio of H2A:Strep-H2A, with equimolar amounts of H2A+Strep-H2A:H2B:H3:H4. Mono-prenucleosomes (with or without Strep-H2A) were incubated for 2 h at 4˚C with Streptavidin-coupled Dynabeads (Life Technologies) in HEG buffer containing 0.1 M KCl. The beads were washed and then eluted with SDS sample buffer. The resulting samples were subjected to SDS-polyacrylamide gel electrophoresis, and the histones were visualized either by silver staining or by western blot analysis with antibodies against H2A.

Mapping of prenucleosomal DNA by primer extension analysis

DNA sequencing ladders were generated by using the Sequenase version 2.0 DNA sequencing kit (USB) with ^{32}P-labeled primers. For DNA sequencing, the fully ligated DNA (250 bp) was PCR amplified, purified, and used as template DNA. For primer extension analyses, the MNase digestion products were used as the template DNA. Primer extension reactions were performed with *E. coli* DNA polymerase I, large (Klenow) fragment (NEB).

Mapping of histone-DNA contacts in the prenucleosome

The labeling of cysteine residues in histones with N-(1,10-phenanthrolin-5-yl)iodoacetamide (OP; Biotium) and the OP-directed cleavage reactions were performed in a manner similar to that described previously (Brogaard et al. 2012; Henikoff et al. 2014). Some specific details are as follows. Wild-type and mutant (H4S47C or H2BT87C) histone preparations (1 mL; 10 μM histone octamers) were dialyzed at 4˚C overnight against TE containing 2 M NaCl, 10 % (v/v) glycerol, and 0.5 mM tris(2-carboxyethyl)phosphine (TCEP). For each set of core histones, the

histones (150 µL; 10 µM histone octamers) and 5 mM TCEP (3 µL) were combined and incubated for 10 min at 22˚C. Next, 4.5 mM OP in DMSO (1 µL) was added to the histone mixture. The reaction was allowed to proceed for 2 h at 22˚C and overnight at 4˚C, and was then terminated by the addition of 2-mercaptoethanol (0.5 µL; 98% purity). The OP-modified histones were dialyzed overnight at 4˚C against TE buffer containing 2 M NaCl, 5 mM 2-mercaptoethanol, and 10% (v/v) glycerol.

The cleavage reactions were performed as follows. Mono-prenucleosomes (reconstituted with OP-labeled histones and 80 bp DNA fragments that were 5'-^{32}P-labeled in the forward strand (Table S1); 1.3 µM mono-prenucleosomes; 40 µL) were combined with Mapping Buffer (40 µL) [0.1 M Tris-HCl (pH 7.5), 5 mM NaCl, and 0.3 mM $CuSO_4$], 60 mM mercaptoproprionic acid (20 µL), 60 mM hydrogen peroxide (20 µL), and Buffer C (80 µL) [50 mM Tris-HCl (pH 7.5), 2.5 mM NaCl] to give a final volume of 200 µL. The reactions were carried out for 20 min at 22˚C, and were terminated by the addition of 25 mM neocuproine (40 µL). The samples were deproteinized, precipitated with ethanol, and analyzed by 10% polyacrylamide-urea gel electrophoresis.

Supplemental References

Brogaard K, Xi L, Wang JP, Widom J. 2012. A map of nucleosome positions in yeast at base-pair resolution. *Nature* **486**: 496-501.

Germond JE, Bellard M, Oudet P, Chambon P. 1976. Stability of nucleosomes in native and reconstituted chromatins. *Nucleic Acids Res* **3**: 3173-3192.

Henikoff S, Ramachandran S, Krassovsky K, Bryson TD, Codomo CA, Brogaard K, Widom J, Wang JP, Henikoff JG. 2014. The budding yeast Centromere DNA Element II wraps a stable Cse4 hemisome in either orientation in vivo. *eLife* **3**: e01861.